QM Degenerate Gases Review

A personal collection of notes in preparation for the lab.

Rachel Wang | No. 23968150

May 2, 2021

Contents

Contents **1**

1 3D Magneto-optical Trap (MOT) **3**
1.1 Doppler Cooling . . . 3
1.1.1 Helmholtz Geometry . . . 3
1.1.2 Anti-Helmholtz Geometry . . . 4
1.1.3 Biot-Savart Law . . . 4
1.2 Zeeman Splitting . . . 6
1.2.1 Landé Factor . . . 7
1.3 MOT Principle . . . 9
1.3.1 Pump and Repump Lasers . . . 10

2 Magnetic Trap (MT) **12**
2.1 Background Information . . . 12
2.1.1 High- and low-field seeking atoms . . . 12
2.1.2 Proof: no local maximum in $|\mathbf{B}|$ . . . 13
2.1.3 Larmor precession . . . 13
2.1.4 Aside: interatomic forces (VdW and the LJ potential) . . . 14
2.1.5 Selection Rules . . . 15
2.2 MT Principle . . . 19
2.2.1 Field strength effects on energy shifts . . . 19
2.2.2 Transition control . . . 19
2.2.3 Trap depth and RF knife . . . 20

3 Trap Dynamics **22**
3.1 MOT Dynamics . . . 22
3.2 MT Dynamics . . . 24
3.3 Background-induced collisional loss . . . 24
3.3.1 Quantum Scattering Theory . . . 25

4 Experimental Apparatus and Methods **27**
4.1 Measurement of $\langle \sigma v_{\mathrm{Ar}} \rangle_{^{87}\mathrm{Rb},^{40}\mathrm{Ar}}$ . . . 27
4.1.1 Γ measurement for a MOT . . . 27
4.1.2 Γ measurement for a MT . . . 29
4.1.3 $\langle \sigma v_{\mathrm{Ar}} \rangle_{^{87}\mathrm{Rb},^{40}\mathrm{Ar}}$ Measurement Data . . . 31

References **33**

Appendix A Quantum Numbers **34**

Appendix B No local field maximum in MTs **34**

Appendix C Deriving the anti-Helmholtz field **36**

Appendix D Solving for $N(t)$ **37**

Appendix E 2-particle scattering **38**

Appendix F Deriving $\langle \sigma_{\text{loss}} v_i \rangle_{X,i}$ **39**

Appendix G *Review:* Spherical Harmonics **40**

Introduction

Atoms can be trapped using light, electric fields, or magnetic fields such that they are suspended in an ultra-high vacuum chamber, spatially confined and isolated from the walls. Collisions with background atoms reduce the sample size and is often an undesired process. However, the *loss rate* can be a useful experimental observable, a measurement of which has many applications (e.g. atomic pressure sensors). The **loss rate constant** Γ depends on the background gas *density* and (velocity-averaged) collisional loss *cross section*. It has units of s^{-1}; therefore the **trap lifetime** is $\tau = 1/\Gamma$.

The **trap species** X is ^{87}Rb and ^{40}Ar is the **background species** i. The average temperature T of the trapped atoms is defined by the average kinetic energy of the atoms $E_k = k_B T$, and is typically in the range of mK to K. The **trap depth** $U_{\text{trap}} = \frac{1}{2}mv_e^2$ where v_e is the minimum trap escape speed. The depth is controlled by parameters of the confining fields, such as light intensity, light frequency, and magnetic field gradient. Certain trap type and depth pairs can reach several K.

1 3D Magneto-optical Trap (MOT)

A 3D magnto-optical trap (MOT) has 3 pairs of counter-propagating along the $\hat{x}, \hat{y}, \hat{z}$ axes. These beam pairs of frequency ω are **detuned** – meaning slightly tuned below **atomic resonance**. Why? Because of the **Doppler effect**. An atom travelling with velocity $\vec{v}$ will see light (with wave vector k and frequency ω) as having a shifted frequency: $\omega' = \omega - \vec{k} \cdot \vec{v}$. The absorption of a photon with wavevector $\vec{k}$ by an atom of velocity $\vec{v}$ will change its momentum by $\hbar\vec{k}$.

$$\begin{cases} \vec{k} \cdot \vec{v} < 0 & = \text{ photons slowing atoms in the intersection (of the triple beam pairs)} \\ \vec{k} \cdot \vec{v} > 0 & = \text{ photons speed up atoms} \end{cases}$$

In the case $\vec{k} \cdot \vec{v} > 0$, ω is shifted further away from resonance, thus having a smaller absorption cross section. Consequently, atoms prefer to absorb 'slowing photons' with $\vec{k} \cdot \vec{v} < 0$. The emission of photons by an atom is spontaneous and in a random direction, meaning the average momentum gain is zero and atoms are slowed.

While on *average* the laser-cooled atoms have $\vec{v} \to 0$, residual motion from absorbing/emitting photons gives a little momentum 'kick'. How then, do we trap the atoms? The trapping force is provided by a **spatially-varying magnetic field**. Combined with **laser cooling**, an ultracold sample of atoms from a vapour or beam can be obtained. The MOT both slows the atoms via laser cooling, and forms the trap via a pair of concentric coils in an anti-Helmholtz configuration (see Fig. 4). We can think of this as a combination of two trapping types:

"momentum trapping" (Doppler cooling) + "position trapping" (magnetic field) = MOT

1.1 Doppler Cooling

Laser cooling cannot provide the (position) trapping force, as it depends on the velocity, not position, of the atoms (which would diffuse out of the crossing point and lost). Instead, the position-dependent trapping force is generated by a pair of identical coaxial coils, separated by their radius R, with equal current I flowing in opposite directions – a geometry colloquially known as '**anti-Helmholtz**' (see §1.1.2).

1.1.1 Helmholtz Geometry

Let's first examine the magnetic field of a pair of Helmholtz coils. This configuration is the standard technique for generating a uniform magnetic field, consisting of a pair of identical coaxial coils with currents I flowing in the same direction. The magnetic field on-axis for a circular current loop of radius R and current I is [1]

$$B(z) = \frac{\mu_0 I R^2}{2\left(R^2 + z^2\right)^{3/2}} \tag{1}$$

at a distance z from the centre of the coil. A nearly uniform field can be produced at the centre ($z = 0$) with two coils spaced by d distance, placed symmetrically above and below the xy-plane (see Fig. 2a). Derived from the **Biot-Savart law**[1] (see §1.1.3), the field as a function of z is

$$B(z) = \frac{\mu_0 I R^2}{2}\left[\frac{1}{\left\{R^2 + \left(z - \frac{d}{2}\right)^2\right\}^{3/2}} + \frac{1}{\left\{R^2 + \left(z + \frac{d}{2}\right)^2\right\}^{3/2}}\right] \tag{2}$$

where $\frac{\partial B}{\partial z}\big|_{z=0} = 0$, due to coil symmetry[2]. For a more uniform field (**Helmholtz condition**), we set $d = R$ such that $\frac{\partial^2 B}{\partial z^2}\big|_{z=0} = 0$ and $\frac{\partial^3 B}{\partial z^3}\big|_{z=0} = 0$ as well. This gives a uniform field over a wide region around the centre, where the magnetic field is $B(0)\big|_{d=R} = \frac{8\mu_0 I}{5^{3/2}R}$. For BEC experiments, the Helmholtz configuration is needed to compensate for a field bias at the trap centre; bias coils provide a uniform axial field at the centre of an Ioffe-Prichard trap and adjust the offset magnetic field of the trap, increasing confinement. (See TRIUMF Report – Trim Coil Project or Appendix B for a more thorough treatment).

1.1.2 Anti-Helmholtz Geometry

If the currents in the two coils (separated by R) are in opposite directions, the arrangement may be referred to as a pair of anti-Helmholtz coils. The field along the axis of symmetry is zero at the point midway between the coils. If atoms move away from the center, for small displacements the magnetic field changes **linearly** in magnitude[3] and induces a **Zeeman shift** in the energy level of the atoms. This means that as an atom moves further from the centre of the trap the transition level in the atom is shifted closer and closer to the detuned laser frequency and it is more probable that the atom will absorb a photon and by conservation of momentum, will receive an impulse back towards the trap.

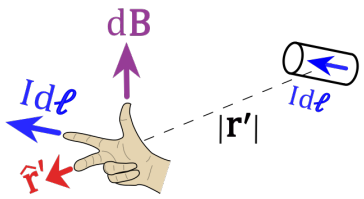

Figure 1: The directions of $d\boldsymbol{\ell}$, $\hat{\mathbf{r}}'$, and the value of $|\mathbf{r}'|$.

There is an **anti-Helmholtz** condition $d = \sqrt{3}R$, for which $\frac{\partial^3 B}{\partial z^3}\big|_{z=0} = 0$. A calculation of the magnetic field B along the z-axis (the axis of symmetry) of a pair of anti-Helmholtz coils yields

$$B(z) = \frac{\mu_0 I R^2}{2}\left[\frac{1}{\left\{R^2 + \left(z - \frac{d}{2}\right)^2\right\}^{3/2}} - \frac{1}{\left\{R^2 + \left(z + \frac{d}{2}\right)^2\right\}^{3/2}}\right] \tag{3}$$

where $+/-$ indicate identical and opposing directions of current flow, respectively. Using anti-Helmholtz coils is the most convenient method of generating these field gradients, which are widely used in magnetic resonance imaging (MRI)[4]. Alkali metal MOTs have field gradients of order 10 G/cm [1] along the symmetry direction. The **maximum field gradient** of B_z is given when $d = R$, which is $\frac{\partial B(0)}{\partial z} = \frac{48\mu_0 I}{25\sqrt{5}R^2} = 2\frac{\partial B_\rho(0)}{\partial \rho}$ (i.e. the axial magnetic field gradient is $2\times$ radial gradient). Thus, for both the Helmholtz and anti-Helmholtz configurations, it is useful to space them by $d = R$ (Fig. 3).

1.1.3 Biot-Savart Law

Recall that the Biot-Savart law takes the form

$$\mathbf{B}(\mathbf{r}) = \frac{\mu_0 I}{4\pi}\int d\mathbf{r}' \times \frac{\mathbf{r} - \mathbf{r}'}{|\mathbf{r} - \mathbf{r}'|^3} \tag{4}$$

[1] An equation describing the magnetic field generated by a constant electric current (source), in a similar manner to how Coulomb's law relates the electric field to a point charge (source).

[2] For this reason, these are sometimes referred to as 'curvature' coils, producing a zero gradient field near the trap centre.

[3] From the azimuthal symmetry of magnetic traps, the minimum will appear on the azimuthal axis at the origin (gravity shifts this downwards). This is in the form $\|\mathbf{B}\| = C\sqrt{x^2 + y^2 + 4z^2}$.

[4] When a sample is placed in a field gradient, the precession frequency of protons in the sample (which depends on $\mathbf{B}$) will vary linearly as a function of position. The precession frequency can be detected and converted into a highly resolved spatial image.

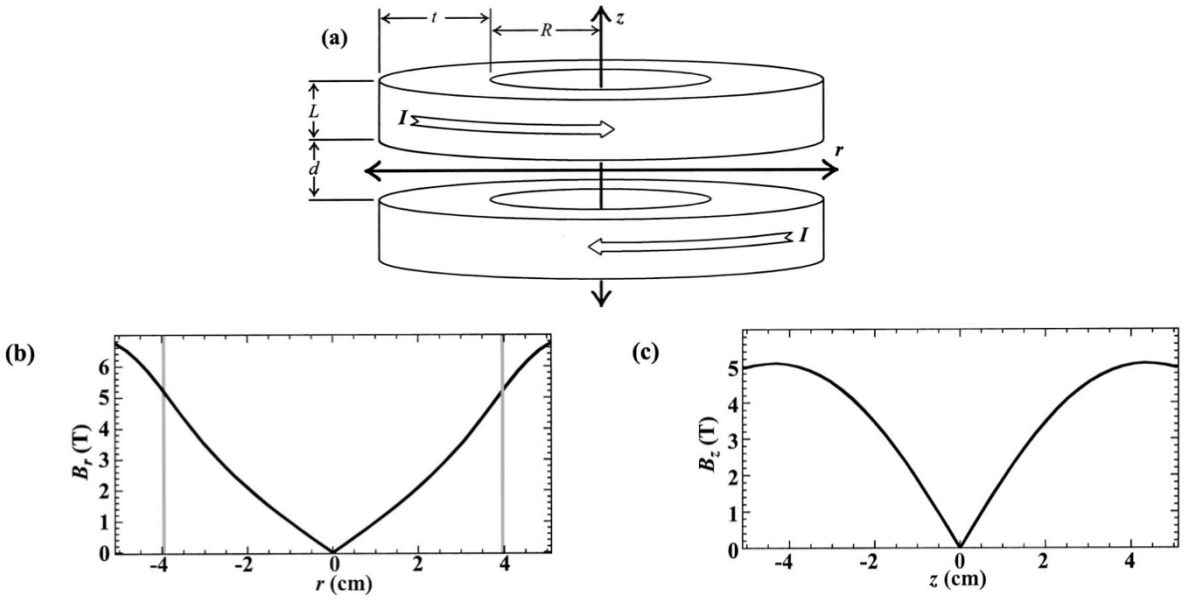

Figure 2: (a) Schematic illustration of the anti-Helmholtz geometry, with coil dimensions t, d, R, and L for each magnet. (b) Plot of $B_r(r, z = 0)$ at maximum current for the experimental setup in [2]. (c) Plot of $B_r(r = 0, z)$ for the same setup.

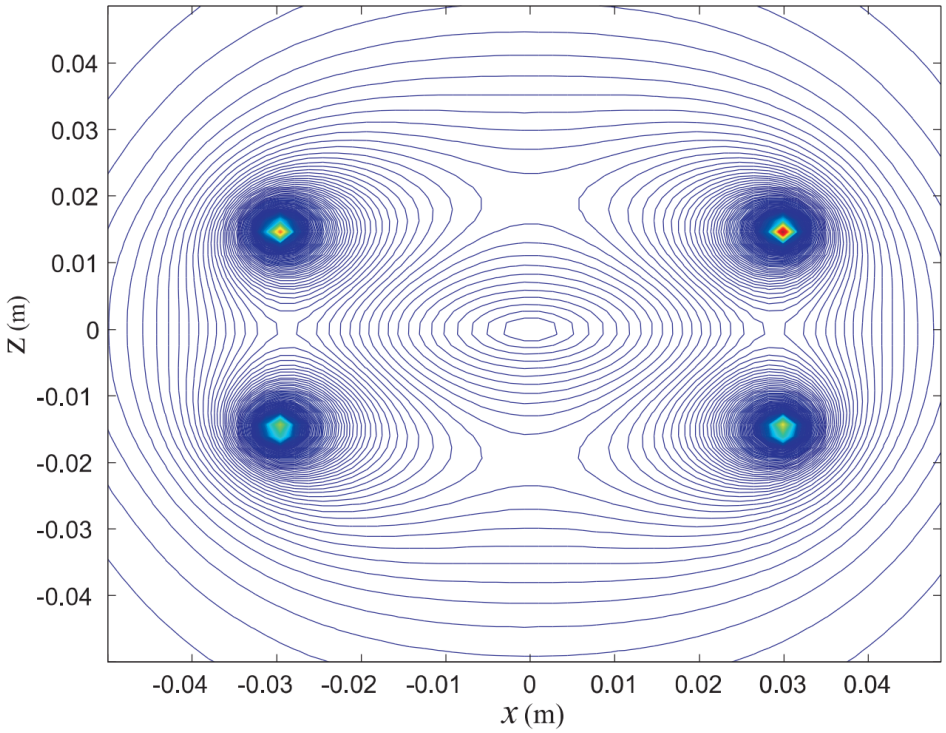

Figure 3: Contour plot of the magnetic field strength produced by the 2 coils on the xz-plane. Recall that the coils are placed symmetrically above and below the xy-plane. The 4 dark regions indicate where the coils emerge from the xz-plane, and the regions with the strongest field strength. This plot was calculated with $I = 200$ A and $d = R = 30$ mm [1].

where the vector $\mathbf{r} - \mathbf{r}'$ is the full displacement vector from some point on the path (line for the 1-dimensional conductor) C to the point where at which the field is being evaluated at $\mathbf{r}$. In vacuum, $\mu_0 = \mu = 4\pi \times 10^{-7}$ H/m (SI units).

Holding the field point fixed (at $\mathbf{r}$), the line integral over the current path gives the total magnetic field at that point. Application of this law implicitly relies on the *superposition* principle – in that, $\mathbf{B}_{\text{tot}}$ is the vector sum of the contributions $d\mathbf{B}$ from each infinitesimal current element. A 2D version of the Biot-Savart law is used when sources are invariant in one direction. In general, the current flow is not necessarily restricted a plane normal to the invariant direction, and is described by the current density $\mathbf{J}$. The 2D form is

$$\mathbf{B}_{2\text{D}}(\mathbf{r}) = \frac{\mu_0}{2\pi} \int_C \frac{(\mathbf{J}d\ell) \times \mathbf{r}'}{|\mathbf{r}'|} = \frac{\mu_0}{2\pi} \int_C (\mathbf{J}d\ell) \times \hat{\mathbf{r}}' \tag{5}$$

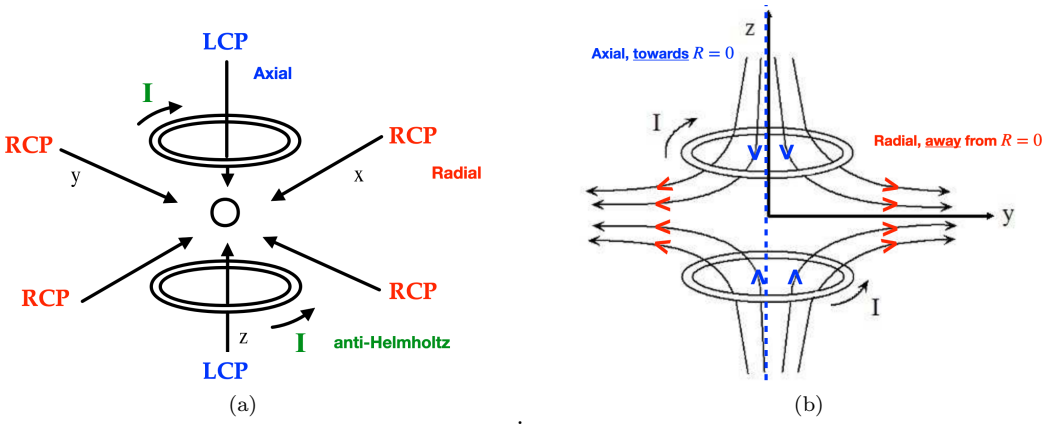

Figure 4: (a): A 3D magneto-optical trap (MOT). Three counter-propagating pairs of beams and magnetic coils in an anti-Helmholtz configuration. Light is RCP for beams travelling along the radial direction, where $\mathbf{B}$ points radially outward. Light is LCP[a] for beams along the axial direction[b], where $\mathbf{B}$ points toward the MOT centre. | (b): A pair of identical coaxial coils, spaced by their radii, whose currents I are equal and flow in opposite directions. The magnetic field produced is $\mathbf{B} = 0$ at the trap centre and increases linearly in magnitude, pointing away from the centre in the radial direction with $\hat{x}$ ($\odot$) and $\hat{y}$, and towards the centre in the axial direction $\hat{z}$ (as $\|\mathbf{B}\| \propto \sqrt{4z^2 + r^2}$).

[a] The light is LCP and not RCP, because the field direction is reversed – it looks 'backwards' to the atoms as the quantization axis is flipped.

[b] The direction concentric with the coil centres is called the axial direction.

1.2 Zeeman Splitting

The **Zeeman effect** is the splitting of spectral lines in the presence of a static *magnetic* field. It is analogous to the **Stark effect**, which is the spectral line splitting in the presence of a static *electric* field. More specifically, Zeeman splitting is attributed to the interaction between the magnetic field and magnetic dipole moment, associated with the orbital angular momentum. Possible transitions are constrained by **selection rules**.

The total Hamiltonian of an atom in a magnetic field is

$$H = H_0 + V_M \qquad \text{where } V_M = -\vec{\mu} \cdot \vec{B} \tag{6}$$

where H_0 is the unperturbed Hamiltonian and V_M is the perturbation due to the magnetic field. The magnetic moment μ of the atom consists of both electric and nuclear parts, though the contribution from the latter is negligible (and is ignored here).

$$\vec{\mu} \approx -\frac{\mu_B g \vec{J}}{\hbar} \qquad \text{(approx.)} \tag{7}$$

where $\mu_B = \frac{e\hbar}{2m_e} \simeq 9.274 \times 10^{-24}$ J $\cdot$ T^{-1} is the **Bohr magneton**[5], $\vec{J}$ is the **total electronic angular momentum**, and g is the **Landé g-factor** (§1.2.1). A more accurate approach is to include the contributions of the **orbital** (azimuthal) and **spin** (intrinsic) **angular momenta**, $\vec{L}$ and $\vec{S}$, respectively

$$\vec{\mu} = -\frac{\mu_B \left(g_L \vec{L} + g_S \vec{S}\right)}{\hbar} \tag{8}$$

where $g_L = 1$ and $g_S \approx 2.0023192$.

The **fine structure** describes the spectral line splitting of atoms due to electronic spin and relativistic corrections to the non-relativistic (NR) Schrödinger equation (SE). The **hyperfine structure** small shifts in otherwise degenerate energy levels, resulting from interactions between the nucleus and electron clouds. More concisely,

Fine structure = due to spin-orbit (S-L) coupling

Total **electronic** (e^-) angular momentum : $\vec{J} = \vec{L} + \vec{S}$ $\qquad |L - S| \leq J \leq |L + S|$

Hyperfine structure = due to coupling of $\vec{J}$ (electronic) with $\vec{I}$ (nuclear angular momentum)

Total **atomic** angular momentum : $\vec{F} = \vec{J} + \vec{I}$ $\qquad |J - I| \leq F \leq J + I$

QM tells us that angular momentum $\vec{J}$ is quantized in **magnitude** $J^2 = \hbar^2 J(J+1)$ and **direction** $J_z = m_z \hbar$. All states that differ only in m_j are $(2J+1)$ degenerate. If an atom is placed in an external $\vec{B}$-field, then a specific direction is created; this **directional quantization** is normally not noticeable in E levels, since $\hat{z}$ is arbitrary (isotropic space). Additionally, while we can't predict the nuclear spin I exactly – protons and neutrons are composed of smaller quarks/gluons – there are rules for the net spin:

$$\begin{aligned} \#n = \text{even and } \#p = \text{even} &\Rightarrow I = 0 \\ \#n + \#p = \text{odd} &\Rightarrow I = \text{half-integer} \\ \#n = \text{even and } \#p = \text{even} &\Rightarrow I = \text{integer} \end{aligned}$$

1.2.1 Landé Factor

A g-factor is a proportionality constant that relates the observed **magnetic moment** μ of a particle, to its **angular momentum quantum number**. Quantum numbers correspond to **eigenvalues** of operators that commute with the Hamiltonian (**conserved** quantities) – quantities that can be known precisely at the same time as the systems energy E and their corresponding **eigenspaces**[6].

The Landé g-factor[7], also known as the **Landé splitting factor**, is a multiplicative term in expressions for the splitting of E levels and controls the scale of the splitting (for an atom in the **weak field limit**, typically $\lesssim 0.001$ T or 10 G [3]). Electrons in atomic orbitals often have degenerate states, sharing the same E and J. In a weak field, this degeneracy is lifted. The factor appears in calculating the first-order **perturbation** in the energy of an atom in a uniform weak[8] field.

$$g_J = g_L \frac{J(J+1) - S(S+1) + L(L+1)}{2J(J+1)} + g_S \frac{J(J+1) + S(S+1) - L(L+1)}{2J(J+1)} \tag{9}$$

where $g_L = 1$ (exact; infinite-mass nucleus $\gg e^-$). Making the assumption $g_s \approx 2$ (approximate; QED effects), this simplifies to

$$g_J\,(g_L = 1, g_S = 2) = \frac{3}{2} + \frac{S(S+1) - L(L+1)}{2J(J+1)} \quad \text{(electronic)} \tag{10}$$

[5] The natural unit of the magnetic moment (of an e^- caused by either its spin or orbital momentum).

[6] Eigenspace is a set of the eigenvectors associated with a specific eigenvalue and $\vec{0}$. An eigenvector does not rotate under a given linear transformation.

[7] A broader use of the term, outside atomic physics, typically treats an electron with both spin and angular momenta.

[8] That is, weak relative to the internal magnetic field of the system.

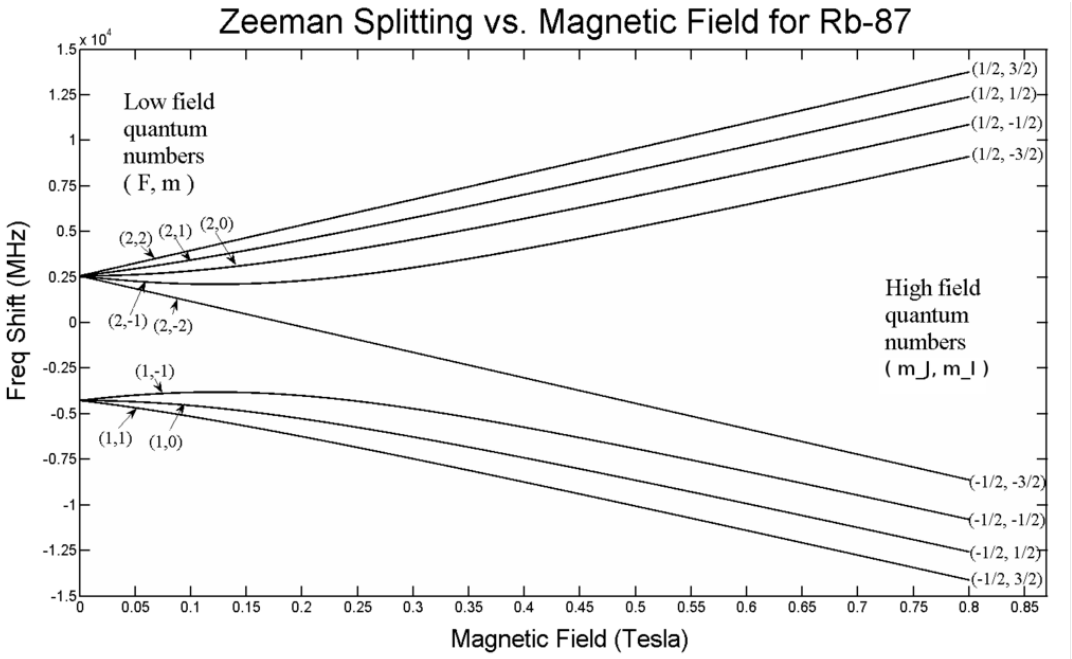

Figure 5: Zeeman splitting of the $5s$ level ^{87}Rb, including fine and hyperfine structure splitting. Here, $F = J + I$ where the nuclear spin $I = \frac{3}{2}$ for ^{87}Rb.

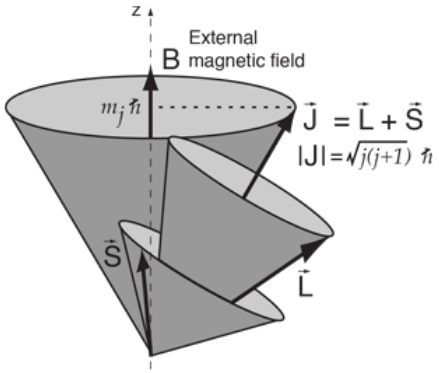

Figure 6: A vector model showing $\vec{L}$ and $\vec{S}$ projections onto the coordinate direction $\vec{J}$.

For an atom with total atomic angular momentum $F = I + J$ (nucleus + electrons), this takes the form

$$\begin{aligned} g_F &= g_J \frac{F(F+1) - I(I+1) + J(J+1)}{2F(F+1)} + g_I \frac{F(F+1) + I(I+1) - J(J+1)}{2F(F+1)} \\ &\approx g_J \frac{F(F+1) - I(I+1) + J(J+1)}{2F(F+1)} \qquad \text{(atomic)} \end{aligned} \tag{11}$$

Since the factor arises in the evaluation of the magnetic interaction (Zeeman effect), the magnetic interaction energy classically is

$$\Delta E = -\vec{\mu} \cdot \vec{B} \quad \text{(classical)} \qquad\qquad \Delta E = \frac{e}{2m}\left(\vec{L} + 2\vec{S}\right) \cdot \vec{B} \quad \text{(quantum)} \tag{12}$$

The problem with evaluating the scalar product is that $\vec{L}$ and $\vec{S}$ continuously change directions (see Fig. 6 above). The strategy for dealing with this is to use the direction of $\vec{J}$ as the **new coordinate direction** and calculate the **projections** of $\vec{L}$ and $\vec{S}$ in the $\hat{J}$ direction. We take the scalar product of each vector, with a unit vector in the $\hat{J}$ direction. To calculate E shifts, this is expressed in terms of

quantum numbers which, in reduced form, is

$$\Delta E = \frac{e}{2m}\frac{\left(L^2 + 2S^2 + 3L\cdot S\right) m_j \hbar B}{J^2} = g_L m_j \mu_B B \tag{13}$$

where

$$\mu_B = \frac{e\hbar}{2m} = 5.78838 \times 10^{-5}\ \text{eV/T} = \text{Bohr magneton} \tag{14}$$

$$g_L = 1 + \frac{j(j+1) + s(s+1) - l(l+1)}{2j(j+1)} = \text{Landé g-factor} \qquad \text{using } J^2 = j(j+1)\hbar \text{ etc.} \tag{15}$$

1.3 MOT Principle

In a MOT the magnetic field in combination with the appropriate polarization choice of the laser beams provides confinement of the atoms. In a MOT atoms preferentially absorb light that pushes them to the trap centre where $\mathbf{B} = 0$.

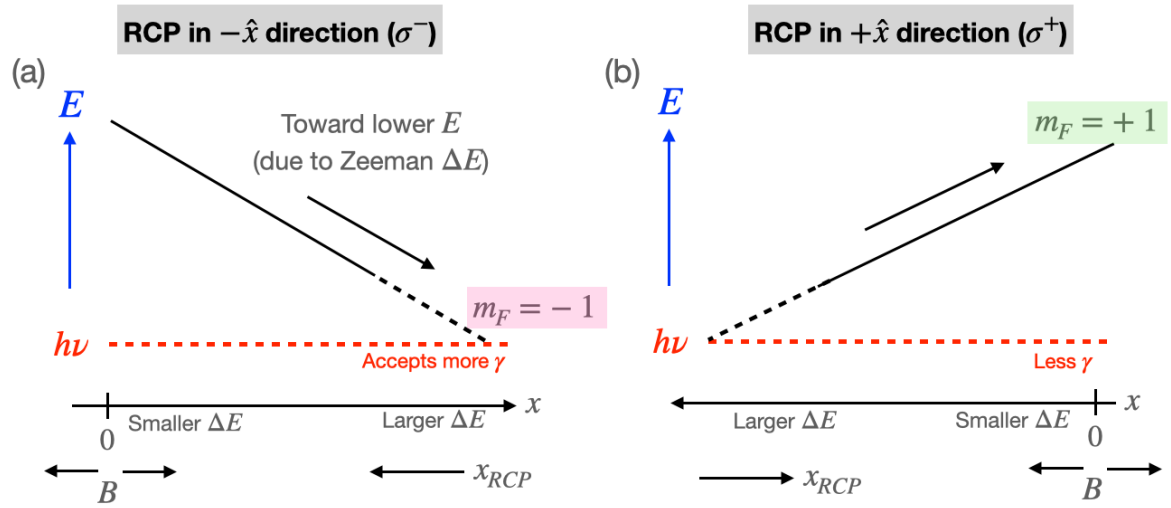

Figure 7: Atoms moving in $+\hat{x}$ with $x > 0$ and $\mathbf{B} = Bx\cdot\hat{x}$. (a) RCP light travels in the $-\hat{x}$ direction, driving σ^- transitions. (b) RCP light travels in the $+\hat{x}$ direction, driving σ^+ transitions (to harder-to-trap states).

Consider laser light that is red detuned below the $F = 0 \rightarrow F' = 1$ transition (resonant ν). In the presence of the weak magnetic field in a MOT, the hyperfine m_F sublevels change as

$$\Delta E = m_F g_L \mu_B B \qquad (g_L = g_F) \tag{16}$$

where in the case $g_{F'} > 0$, the $m_{F'} = -1$ transition $\downarrow E$ away from the $\mathbf{B} = 0$ position.

In the **radial direction**, RCP light propagating in the same direction as $\vec{B}$ will drive $\Delta m_F = m_{F'} - m_F = -1$ or σ^- transitions (Fig. 7a). In case (a) the atom's E tends toward resonance and accepts more photons (a stronger push to $R = 0$; the effect is more pronounced as $\uparrow R$ and $\uparrow B$). In case (b), atoms are ejected by the RCP light alignment with the field in σ^- transitions (Fig. 7b). If the RCP light is propagating in the opposite direction, it drives $\Delta m_F = m_{F'} - m_F = +1$ or σ^+ transitions. In Fig. 8, the transition closest to the laser frequency (dotted line) is the $m_F = 0 \rightarrow m_{F'} = -1$ transition.

In the **z direction**, LCP light must be used. The alignment of LCP light w.r.t the magnetic field will drive $\Delta m_F = -1$ (aligned) and $\Delta = +1$ (anti-aligned) transitions.

Q: Why choose rubidium-87 as the trapped species?
For experiments involving magnetic trapping, it is more convenient to use ^{87}Rb to trap atoms

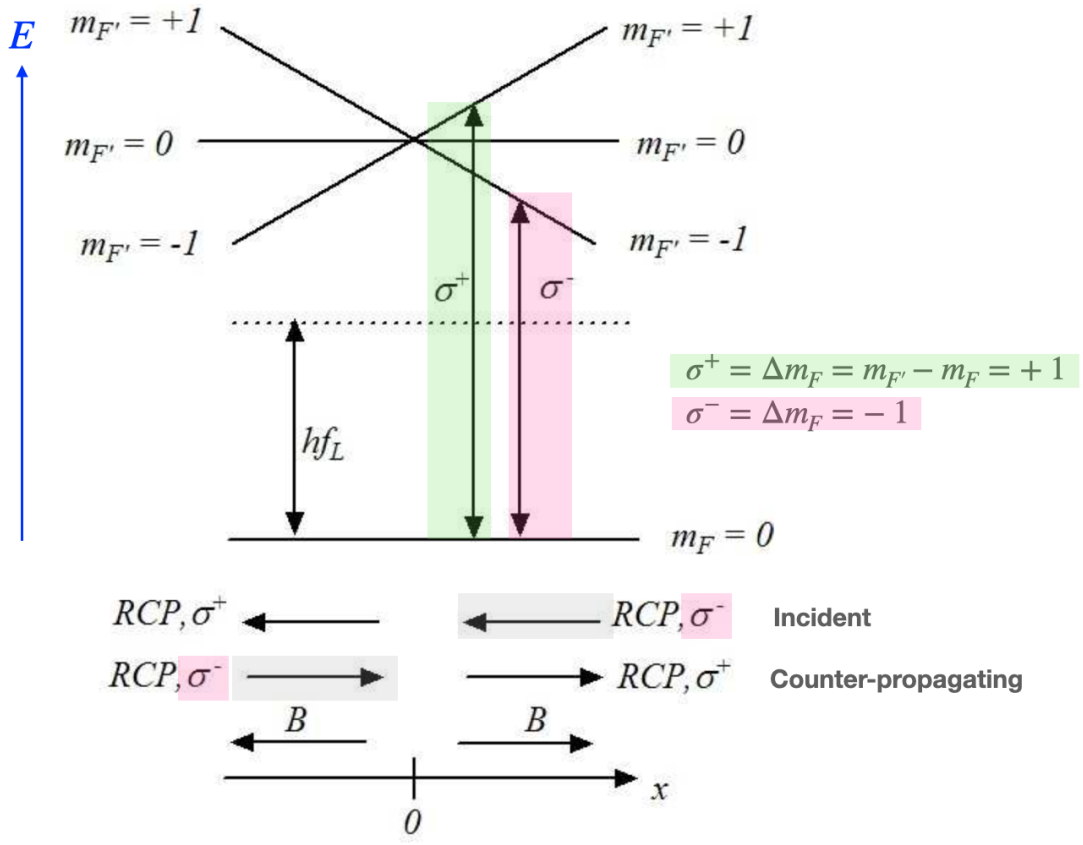

Figure 8: Hyperfine sublevels undergoing a continuous energy shift (solid lines) when subjected to a spatially-varying magnetic field in the trap. The $m_F = 0 \rightarrow m_{F'} = -1$ transition is closest to the laser frequency (dotted line), so the atoms preferentially absorb σ^- light. Atoms on either side of the magnetic zero ($\pm\hat{x}$) have a greater probability of absorbing σ^- light, which pushes atoms back to the magnetic zero.

Radial Axes	RCP	Δm_F	ẑ-axis	LCP	Δm_F
$\sigma+$	$\uparrow\uparrow B$	$+1$	σ^+	$\downarrow\uparrow B$	$+1$
σ^-	$\downarrow\uparrow B$	-1	$\sigma-$	$\uparrow\uparrow B$	-1

Table 1: CP light and their associated transitions based on field and quantization axis orientation.

all in the same hyperfine sublevel. In general, the choice of the atom species is a practical one, relying on the availability of the laser for each species.

1.3.1 Pump and Repump Lasers

Laser light used for trapping in the MOT is called the **pump light**. A secondary laser, called the **repump light**, is needed to prevent atoms from transitioning to and remaining in a sublevel that is inaccessible to the pump laser – i.e. it cannot be excited. The transition chosen for both the pump and repump light is the $5^2S_{1/2} \rightarrow 5^2P_{3/2}$ transition (see Appendix A). For ^{87}Rb, the **pump** laser is resonant with the $F = 2 \rightarrow F' = 3$ transition and the **repump** is resonant with the $F = 1 \rightarrow F' = 2$ transition (see Table 2).

What about **off-resonance** transitions? The same $F = 2 \rightarrow F' = 3$ transition may also drive the off-resonance transitions to the $F' = 2$ or $F' = 1$ hyperfine levels as well. These levels can decay to the $F = 1$ hyperfine level of the $5^2S_{1/2}$ GS – we call this the **'dark' state**. In this state, atoms will not strongly absorb pump light any more, so it is 'dark' in the sense that laser cooling/trapping is not achieved. The repump light drives the $F = 1 \rightarrow F' = 2$ transition to ensure that there is *some* probability of the atoms

decaying to the $F = 2$ state. Numerical values for Figs. 10 and 9 are from [4] and [5] respectively.

Note: we've been referring to **D_2 transitions** a lot, but what is it?

Designation of D-transitions between the GS and 1st ES of Alkali Atoms

$$\left.\begin{array}{ll} D_1 - transition: & 5^2S_{1/2} \rightarrow 5^2P_{1/2} \\ D_2 - transition: & 5^2S_{1/2} \rightarrow 5^2P_{3/2} \end{array}\right\} = \begin{array}{c}\textbf{Fraunhofer Lines} \\ \text{(Fine structure splitting of ES)}\end{array}$$

Species	Transitions	
	Pump	Repump
^{87}Rb	$F = 2 \rightarrow F' = 3$	$F = 1 \rightarrow F' = 2$
^{85}Rb	$F = 3 \rightarrow F' = 4$	$F = 2 \rightarrow F' = 3$

Table 2: A summary of the ^{87}Rb resonance transitions for the pump and repump lasers.

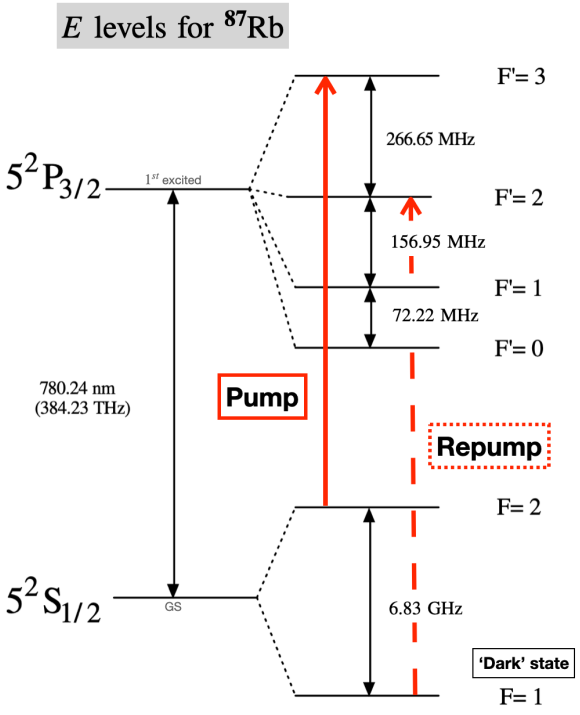

Figure 9: E levels for the D_2 transition of ^{87}Rb.

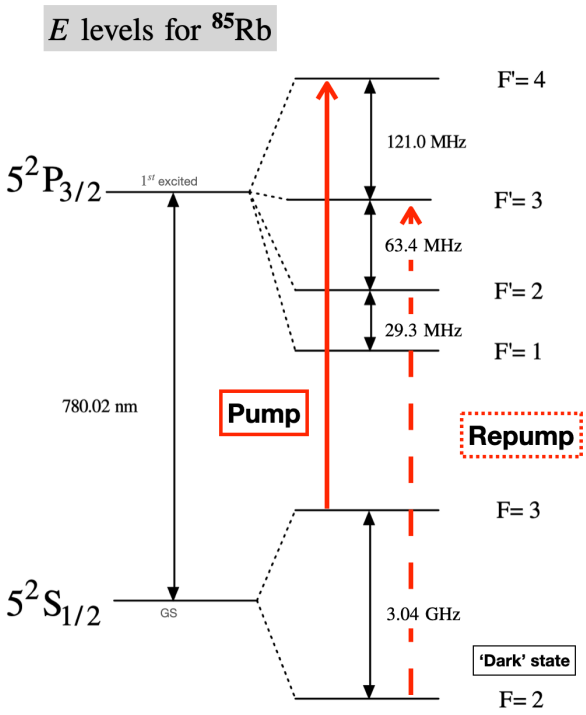

Figure 10: E levels for the D_2 transition of ^{85}Rb.

2 Magnetic Trap (MT)

After atoms are cooled and trapped in the MOT, they can be transferred to a magnetic trap (MT) for further study or cooling. A **quadrupole** MT can be formed using the same coils as for the MOT – though this time with a **higher current** to produce a greater magnetic field gradient; the laser light is also turned off.

> Q: Why do we need **both** the MOT and MT?
> The initial cooling stage in the MOT is necessary, because MTs do not provide cooling and offer weak trapping forces for confinement. In short, MTs are bad at cooling and trapping atoms.

2.1 Background Information

Consider an electron with spin $\vec{S}$, electronic angular momentum $\vec{L}$, and nuclear spin $\vec{I}$, interacting with a magnetic field. This adds to the total Hamiltonian (Eqn. 6):

$$H_B = \frac{\mu_B}{\hbar}\left(g_S\vec{S} + g_L\vec{L} + g_I\vec{I}\right)\cdot\vec{B} \tag{17}$$

where again $\mu_B = 9.274\times10^{-24}$ J/T and $g_i,\ i = S, L, I$ are the spin, orbital, and nuclear g-factors. For weak magnetic fields, H_B is a perturbation of the hyperfine levels, changing by $\Delta E = g_F m_F \mu_B B$.

2.1.1 High- and low-field seeking atoms

Consider atoms in a MT, with a magnetic gradient superimposed onto a uniform field. We claim the following:

"$m_F = -1$ is an **untrappable state** (or at least hard-to-trap)."

(a) **High-field seeking atoms (MT)**: $\uparrow\uparrow \,\big|\, \uparrow \vec{B} \,\big|\, \downarrow E$
Atoms want occupy the ('new') lowest E states (pertaining to the imposed field gradient). To do so, they must tend toward regions with higher $\vec{B}$ strength, as the ΔE they lose to the Zeeman interaction is $\Delta E \propto \vec{B}$. In other words, atoms whose magnetic moments are aligned $\uparrow\uparrow$ with the field will have lower $\downarrow E$ in a higher $\uparrow \vec{B}$.

(b) **Low-field seeking atoms (MT)**: $\uparrow\downarrow \,\big|\, \downarrow \vec{B} \,\big|\, \downarrow E$
To $\downarrow E$, these atoms must tend toward regions with lower field strength; they lose ΔE to the Zeeman effect at a slower rate as $R \to 0$. This can be rephrased as anti-aligned atoms will have higher energies in a higher field.

(c) **Tumbling atoms (MT)**
In reality, both the (total) electronic angular momentum (L, S) and atomic angular momentum (J, I) are constantly changing (see §2.1.3 and Fig. 12). Thus, atoms act more like a pendulum, switching between high- and low-field seeking states.

(d) **Untrapped atoms (MT)**
These atoms are not trapped at $m_F = 0$ because $\Delta E \propto m_F$, meaning it doesn't interact with the $\vec{B}$-field and atoms fly out of the trap.

All of the above (a,b,c,d) are in reference to the subfigures in Figure 11.

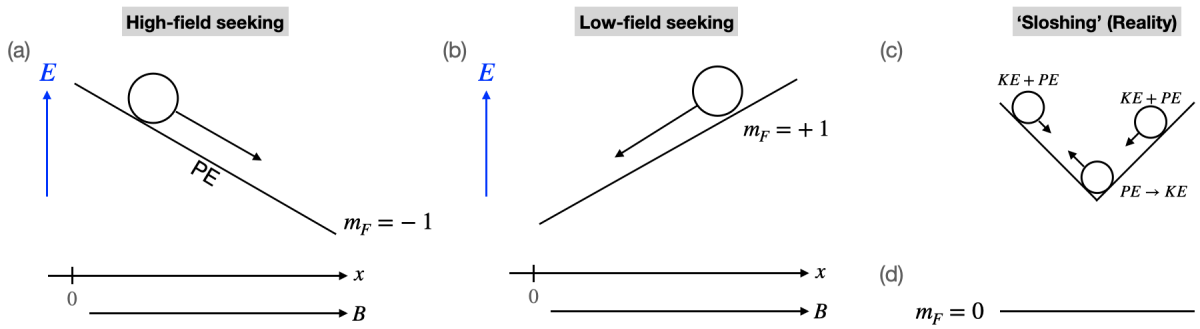

Figure 11: Various configurations for field-seeking atoms. (a) high-fields accelerate the loss of ΔE, so these atoms tend to areas of high $\vec{B}$. (b) low-fields decelerate the loss, so these atoms tend to low $\vec{B}$.

2.1.2 Proof: no local maximum in |B|

We also make the claim:

> "It is **impossible** to produce a **local maximum** of $|\vec{B}|$ in free space; however, a local minima may be produced."

A stationary point is a local maximum of all the eigenvalues of the Hessian matrix are all negative. The **trace** of the Hessian is the **Laplacian**; thus, we want to determine the Laplacian of the **magnetic field magnitude**:

$$\begin{aligned}\nabla^2\mathbf{B}^2 &= \nabla\cdot\nabla({\mathbf{B}_x}^2+{\mathbf{B}_y}^2+{\mathbf{B}_z}^2)\\ &= 2\left[(\nabla\mathbf{B}_x)^2+(\nabla\mathbf{B}_y)^2+(\nabla\mathbf{B}_z)^2+\mathbf{B}_x\nabla^2\mathbf{B}_x+\mathbf{B}_y\nabla^2\mathbf{B}_y+\mathbf{B}_z\nabla^2\mathbf{B}_z\right]\end{aligned} \tag{18}$$

For a time-independent (T.I.) current-free system, we know that $\nabla\times\mathbf{B}=0$. If we take the curl of both sides, we see that

$$\nabla\times\nabla\times\mathbf{B}=0=-\nabla^2\mathbf{B}+\nabla(\nabla\cdot\mathbf{B})$$

Since $\nabla\cdot\mathbf{B}=0$ also, then we can say that $\nabla^2\mathbf{B}=0$, and similarly for the individual components $\nabla^2\mathbf{B}^2=2(\nabla\mathbf{B}_x)^2+(\nabla\mathbf{B}_y)^2+(\nabla\mathbf{B}_z)^2=0$.

Revisiting our work in (18), the following is then true

$$\nabla^2\mathbf{B}^2=2(\nabla\mathbf{B}_x)^2+(\nabla\mathbf{B}_y)^2+(\nabla\mathbf{B}_z)^2$$

Finally, because the square of the individual gradients must always be ≥ 0, we can say that

$$\nabla^2\mathbf{B}^2\geq 0 \tag{19}$$

Therefore, we can say that while a local minimum in $|\mathbf{B}|$ is possible, because tr(Hessian) > 0, it is **impossible** to have a local maximum in $|\mathbf{B}|$, because it can never be < 0.

See Appendix B for further discussion (related theorems and proofs can be found here).

2.1.3 Larmor precession

As we saw in Fig. 6, the momenta S and L are constantly changing as they precess about J. In this vector model, the 'vector' is a projection along the J direction, quantized to values **one unit** of angular momentum apart.

For $\vec{L}$, the possible values (and also maximum number) for this unit (of projected angular momentum) are defined by l (**orbital quantum number**). Since there is a magnetic moment (controlled by m_l (**magnetic quantum number**)) associated with the orbital angular momentum, the precession can be

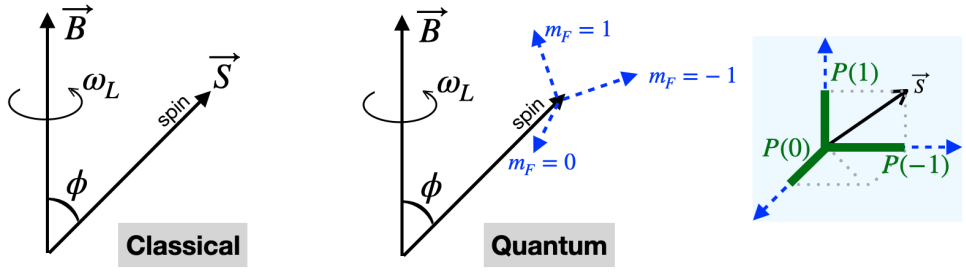

Figure 12: Classical and quantum Larmor precession. ϕ is the precession angle.

compared to **Larmor precession**, with a characteristic **Larmor frequency**, ω_L (see Figs. 12 and 13).

- **Principal quantum number** (n) – describes the electron shell (E level) of an electron.

$$n = 1, 2, 3, \ldots \qquad n \neq 0 \text{ and } l \leq n$$

- **Orbital quantum number** (l) – also called the **angular** or **azimuthal** quantum number, describes the subshell (shape) and gives the **magnitude** of the orbital angular momentum.

$$L^2 = \hbar^2 l(l+1) \quad \text{with} \quad l = 0, 1, 2, \ldots, (n-1) \quad \text{(integer steps)} \quad \text{and } 0 \leq l \leq (n-1)$$
$$= s, p, d, f, \ldots \text{etc.} \qquad \text{(orbitals)}$$

- **Magnetic quantum number** (m_l) – describes the specific orbital (or 'cloud') within that subshell (orientation), and yields the *projection* of $\vec{L}$ along a specified axis (usually $\vec{J}$).

$$L_z = m_l \hbar \quad \text{with} \quad m_l = -l, \ldots, -1, 0, 1, \ldots, l$$

- **Spin quantum number** (m_s or s) – describes the intrinsic spin angular momentum of the electron within each orbital and gives the projection of $\vec{S}$ along the specified axis.

$$S_z = m_s \hbar \quad \text{with} \quad m_s = -s, (-s+1), (-s+2), \ldots, (s-2), (s-1), s$$

See Appendix A for more details on the rubidium transitions.

Q: The nEDM is $d_n \neq 0$ as it has an inhomogeneous charge distribution. Why can we use a MOT to trap neutrons? Why not use a Penning trap (for charged particles)?
In an experimental context, $|d_n| \sim 10^{-26} e\text{cm}$ is too small for this system to measure. A more thorough (and satisfying) answer can be found in the following section.

2.1.4 Aside: interatomic forces (VdW and the LJ potential)

Collisions between atoms are low in energy, so they don't probe the interior structure of atoms (to access and 'see' this inhomogeneity). Long-range interactions between atoms are well-approximated by **Van der Waals** (VdW) forces, of which there are two types:

1. *London dispersion forces* (weakest[9]; LDF) – a type of force acting between atoms and molecules that normally have charge symmetry[10]. For this reason, they are also known as *induced dipole-dipole forces*. Here, electrons in two adjacent atoms form temporary dipoles, and are often found in halogens (e.g. F_2, I_2), noble gases (e.g. Ne, Ar), and other non-polar molecules.

[9] These weak/strong qualifiers are in reference to the strength of intermolecular attractive forces.
[10] In reference to symmetrically distributed electrons w.r.t the nucleus.

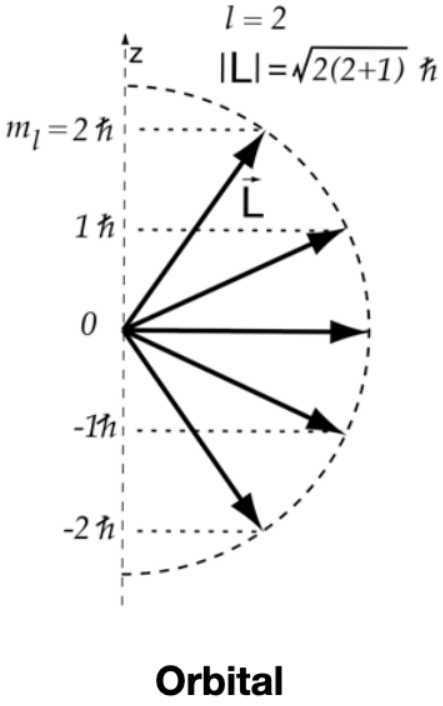

Figure 13: A 'vector' projection of the angular momentum along the $\vec{J}$ direction, in a weak magnetic field. This diagram shows $m_l = -2, -1, 0, 1, 2$ for $l = 2$.

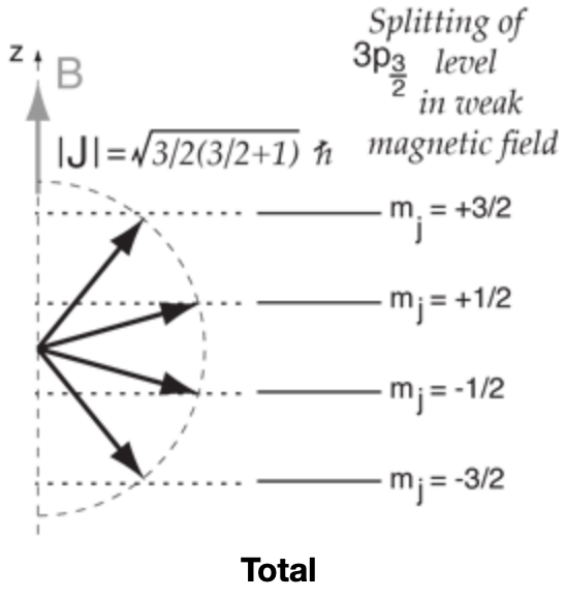

Figure 14: The total angular momentum, combining both the orbital and spin momenta. The problem of $\vec{S}$ and $\vec{L}$ constantly changing as they precess about $\vec{J}$ is handled by the Landé g-factor (§1.2.1). This is a useful model for the Zeeman effect, as the magnetic energy contribution is proportional to the component of $\vec{J}$ along the direction of $\vec{B}$ (usually $\hat{z}$).

2. *Dipole-dipole forces* (strongest; IMF) – are electrostatic interactions between molecules which have permanent dipoles. While much stronger than LDFs, they are weaker than ion-ion interactions as they only involve partial charges. These interactions tend to align molecules to reduce **potential energy** (re: increase attraction).

The **Lennard-Jones potential** (or 12-6 potential; Fig. 15) describes an intermolecular pair potential, as a function of the distance between the two particle centres.

$$V_{\mathrm{LJ}} = 4\epsilon\Big[\cancelto{0}{\frac{c^{12}}{r^{12}}} - \frac{c^6}{r^6}\Big] \tag{20}$$

where r is the interatomic distance, ϵ is the depth of the potential well (i.e. the dispersion energy), and σ is the distance at which the particle-particle potential energy V is zero (i.e. the particle's size).

2.1.5 Selection Rules

There are some states, called **forbidden states**, that atoms (in this case) is not allowed based on a particular selection rule; however, it is allowed with **higher-order approximations**, and will transition to these states at a low rate. For example, the electric dipole approximation is commonly used, and so transitions are strictly forbidden. If a higher approximation is used, such as the electric quadrupole, these blocked transitions are now allowed at a low rate. In other words, forbidden transitions can occur, with a small probability, so long as any approximations made are sufficiently accurate. This probability is the **transition probability**.

Let's take a look at the rules for a rubidium atom. Using the **Born–Oppenheimer (BO) approximation**, we can treat the **wave functions (w.f.)** of atomic nuclei and electrons separately (re: neglect cross-terms), based on the fact that nuclei are much heavier than electrons. (*Phew!*) This separation[11]

[11] We remind ourselves that the multiplication $\psi_1 \otimes \psi_2$ is the tensor product as we're combining probabilities (of two

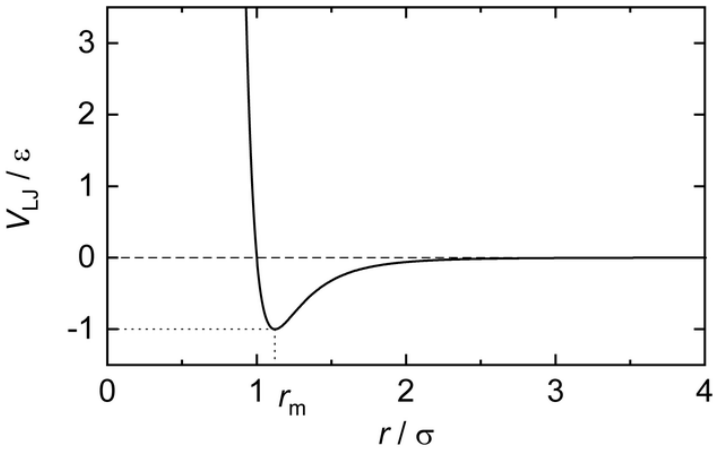

Figure 15: The Lennard-Jones potential, showing the intermolecular potential energy V_{LJ} as a function of the distance of a pair of particles. The potential minimum is at $r = r_m = 2^{1/6}\sigma$, where $V = -\epsilon$.

looks like

$$\Psi_{\text{total}} = \psi_{\text{electronic}} + \psi_{\text{nuclear}} = \Psi(\mathbf{r}, \mathbf{R}) = \psi_e(\mathbf{r}, \mathbf{R})\psi_v(\mathbf{R})\psi_r(\mathbf{R}) \tag{21}$$

where $\mathbf{r}$ and $\mathbf{R}$ represent all electronic and nuclear coordinates, respectively. The subscripts e, v, r represent the electronic, vibrational, and rotational parts.

Brief review: separable Hamiltonian
Let's take a look at the Hamiltonian for the system, noting that electron-nucleus interactions aren't completely removed and the e^-still feels the 'clamped'[a] Coulomb potential. This is great for describing the system, but we're concerned with transitions. We're dealing with 2 coordinates, the electronic and nuclear ones (which we'll just call 1 and 2)

$$H_{\text{tot}} = H_1 + H_2 \qquad (H_1 + H_2)\psi(q_1, q_2) = (E_1 + E_2)\psi(q_1, q_2) \quad \text{(S.E.)}$$

We know that if a Hamiltonian is separable into two or more terms, then the total eigenfunctions are products of the individual eigenfunctions of the separated Hamiltonian terms, and the total eigenvalues are sums of individual eigenvalues of the separated Hamiltonian terms.

If we take a closer look at the electronic portion of the total w.f. (Eqn. 21), and express it as a moment integral (which we'll call M for brevity)

$$M = \iint \psi_e^2(\mathbf{r}, \mathbf{R}_*) \cdot \psi_v^2(\mathbf{R})(\mu_e + \mu_n)\psi_e^1(\mathbf{r}, \mathbf{R}_*) \cdot \psi_v^1 dr dR$$

where $\mathbf{R}_*$ represents the electronic coordinates w.r.t. equilibrium/fixed nuclear coordinates. So, both the e and n components contribute to the operator. Orthonormality of different ψ_e tells us $\int \psi_e^2(\mathbf{r}, \mathbf{R}_*)\psi_e^1(\mathbf{r}, \mathbf{R}_*)dr = 0$ (a term from IBP). Thus, the simplified integral is as such:

$$M = \int \psi_e^2(\mathbf{r}, \mathbf{R}_*) \cdot \mu_e \cdot \psi_e^1(\mathbf{r}, \mathbf{R}_*)dr \int \psi_v^2(\mathbf{R}) \cdot \psi_v^1(\mathbf{R})dR \tag{22}$$

The first integral in Eqn. 22 defines the **electronic selection rules** and the second integral is the basis of **vibrational selection rules**.

[a]For this reason, the first step of the BO approximation is also sometimes referred to as the clamped-nuclei approximation.

uncorrelated particles). For something like a spin state, $|\uparrow\rangle + |\downarrow\rangle$ uses addition in the 'either or' sense.

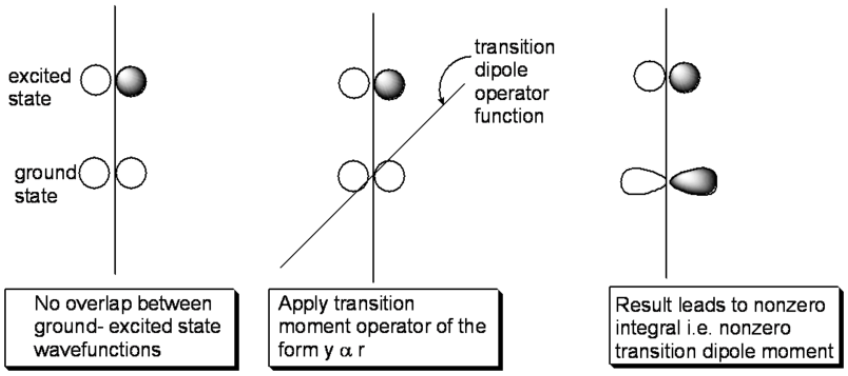

Figure 16: The GS and ES w.f.s must not have the same symmetry if the application of the transition moment operator is to return non-zero.

A natural question that arises is "what is the probability that my atom will absorb light?" This is especially relevant if we want to control specific transitions. A useful quantity is the **transition dipole moment** ($\mu^2_{1,2}$), which can help us predict whether the transition to the excited state (we are interested in GS $\rightarrow 1^{st}$ES) is possible or likely.

In *classical electrostatics*, the dot product of a dipole moment $\vec{\mu}$ with $\vec{E}$ gives the interaction energy (i.e. energy $= \vec{E} \cdot \vec{\mu}$). The total dipole moment is the sum of all the individual μ-vectors

$$\mu_{\text{tot}} = \sum_n e_n \Delta q_n r_n \tag{23}$$

where e is the elementary charge ($\pm$), Δq_n is the fractional charge, and r_n is the particle distance from the reference point. We see that the total moment relies on the **distance** between the charges and their **spatial distribution**. Clearly, we can relate this to the QM description by using the **wave function** (and its associated **probability**) to keep track of those charges; we keep the distance r for determining the moment.

Consider an atom subject to an EM wave, with an induced dipole moment whose frequency matches the ΔE between ψ_1 and ψ_2, the interaction is **resonant** (same ν). Then, $\mu^2_{1,2}$ from one state to another, $\psi_1 \rightarrow \psi_2$, is (if transitioning from the ground to excited state),

$$\mu^2_{g,e} \propto \left| \int \psi_g{}^*(R) \psi_e d\tau \right|^2 \qquad R = e_n r_n$$

Imagine a transition from a state (e.g. GS) to itself. You would have an $\int$ with R sandwiched by the GS and its complex conjugate; you are left with this $\int$ over all space – the dipole moment. It should be clear that, since R is odd, if the GS and ES w.fs are even or odd, they must not have the same symmetry if the $\int$ is to be non-zero (see Fig. 16).

Atomic term symbols are written in the form $\boxed{^{2S+1}L_J}$. When writing the electronic configuration of an atomic species, there are 3 rules we must obey:

1. **Aufbau Principle** – the 'building up' principle, stating that e^-s occupy orbitals in order of increasing energy.
2. **Hund's Rule** – when e^-s occupy degenerate orbitals (same n and l), they must first occupy the empty orbitals before double-occupying them.
3. **Pauli-Exclusion** – each e^-can be described with a unique set of 4 quantum numbers. Thus, if 2 e^-s occupy the same orbital, their spins must be paired ($\uparrow\downarrow$). These electrons would share principal (n), orbital (l) and magnetic (m_l) QM#s, but would differ in spin ($m_s = \pm\frac{1}{2}$).

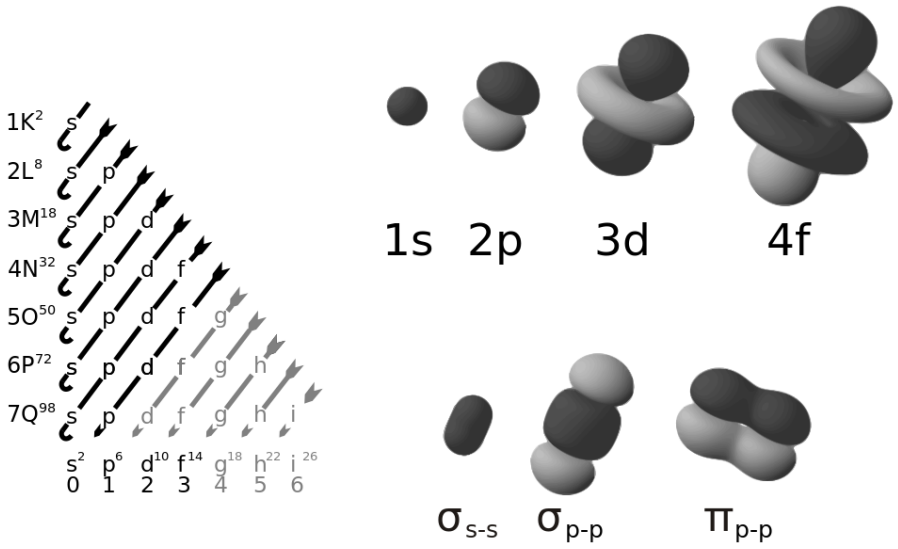

$$1s^2_2\,2s^2_4 2p^6_{10}\,3s^2_{12}\,3p^6_{18}\,4s^2_{20}\,3d^{10}_{30}\,4p^6_{36}\,5s^2_{38}\,4d^{10}_{48}\,5p^6_{54}\,6s^2_{56}\,4f^{14}_{70}\,5d^{10}_{80}\,6p^6_{86}\,7s^2_{88}\,5f^{14}_{102}\,6d^{10}_{112}\,7p^6_{118}$$

Figure 17: Electron and molecular orbitals and the Aufbau principle. Vertically increasing $\downarrow$ is $n = 1, 2, 3, \ldots$ and horizontally increasing $\rightarrow$ is $l = 0, 1, 2, 3, \ldots$. The orbital energy is $E = n + l$.

Let's say we are interested in writing the term symbol for the ground state. We look at the state with maximum S and L, now in the form[12]

$$\textbf{GS term symbol} \;=\; {}^{2\cdot\max(S)+1}\max(L)_J \qquad J = L + S$$

For a spin-$\frac{1}{2}$ particle like e^-s, the maximum S is $\frac{1}{2} \times$ (# of unpaired e^-s). The overall L is calculated by adding the m_l values for each electron[13]. We remind ourselves of the rules for quantum numbers (§2.1.3).

For ^{87}Rb, looking at the periodic table its electronic configuration is $1s^2 2s^2 2p^6 3s^2 3p^6 4s^2 3d^{10} 4p^6 \underline{\mathbf{5s^1}}$. Its relevant quantum numbers are: $n = 5$, $l = 0 = s$, $\max(m_l) = +l = 0$, and $\max(m_s) = +s = \frac{1}{2}$. If $J = L + S = 0 + \frac{1}{2} = \frac{1}{2}$, then the GS term symbol for ^{87}Rb looks like

$$\text{GS for the } {}^{87}\text{Rb } n = 5 \text{ state} \quad \Rightarrow \quad {}^{2\cdot\frac{1}{2}+1}S_{\frac{1}{2}} = 5^2S_{1/2}$$

For the $1st$ ES of ^{87}Rb, selection rules tell us that we must obey

$$\Delta S = 0 \quad \text{and} \quad \Delta L = \pm 1 \qquad \text{but} \quad L = 0 \nleftrightarrow 0$$

for a single electron jump. The convention is to use $\nleftrightarrow$ to represent a forbidden transition. So, the QM#s that change are $l = 0 \rightarrow 1$ and consequently $J + (L + 1) + S = \frac{3}{2}$, which looks like

$$1^{st} \text{ ES for the } {}^{87}\text{Rb } n = 5 \text{ state} \quad \Rightarrow \quad {}^{2\cdot\frac{1}{2}+1}P_{\frac{3}{2}} = 5^2P_{3/2}$$

s^2_2	s^2_4	$2p^6_{10}$	$3\ s^2_{12}$	$3p^6_{18}$	$4\ s^2_{20}$	$3\ d^{10}_{30}$	$4p^6_{36}$	$5\ s^2_{38}$	$4\ d^{105}_{48}$	$5p^6_{54}$	$6\ s^2_{56}$	$4f^{14}_{70}$
d^{10}_{80}	$6p^6_{86}$	$7\ S^2_{88}$	$5f^{14}_{102}$	$6\ d^{10}_{112}7$	p^6_{118}							

[12] We start with the most stable configuration. As full shells and subshells do not contribute to the overall angular momentum, they are ignored

[13] This includes the multiplicity of double-occupied states.

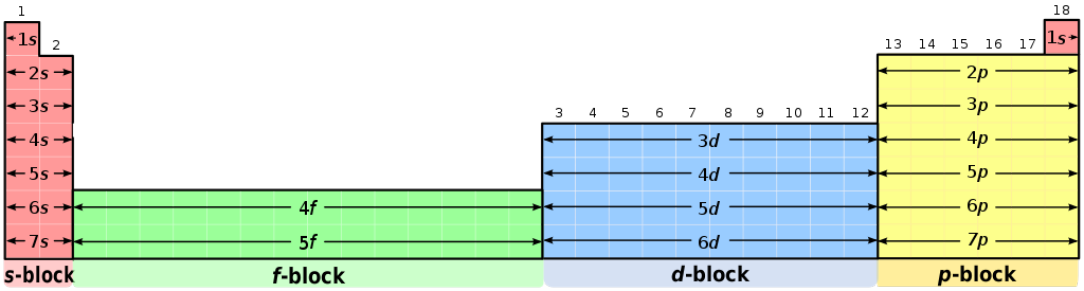

Figure 18: $s-$, $p-$, $d-$, and $f-$blocks in the periodic table.

2.2 MT Principle

2.2.1 Field strength effects on energy shifts

Now, recall Eqn. 17, which we will re-iterate here

$$H_B = \frac{\mu_B}{\hbar}\left(g_S\vec{S} + g_L\vec{L} + g_I\vec{I}\right)\cdot\vec{B}$$

Atoms have trappable (and untrappable) states (§2.1.1), and their behaviour is sensitive to the perturbation H_B to the hyperfine levels (ΔE). Note that $\Delta E = g_F m_F \mu_B B$ only holds for weak-fields (which we defined as $\lesssim 0.001$ T or $\lesssim 10$ G in §1.2.1.). For larger fields, where the H_B term is comparable to the hyperfine term, the two together are a perturbation on the fine structure states. Consequently, our expression ΔE must change. For $J = \frac{1}{2}$ (our case), it is given by the **Breit-Rabi** formula [3]. The field strength affects the splitting

- **Large fields** – H_B perturbs the fine structure, causing a shift $\Delta E = g_J m_J \mu_B B$. The hyperfine term further peturbs these fine structure states. For different m_I values, we see different splitting and ΔE shifts. This is nicely presented in Fig. 5.
- **Weak fields** – ΔE is linear with $|\mathbf{B}|$.
- **Intermediate fields** – ΔE can change non-linearly with $|\mathbf{B}|$. Furthermore, states that were low-field seeking can become high-field seeking and vice versa. For sufficiently large fields, this is important when determining trap depth or potentially trappable states.

* The work done by [6] worked primarily in the weak to intermediate regime, typically up to a maximum of 400 G.

2.2.2 Transition control

Consider the trappable states presented in Table 3 for ^{87}Rb. We see that there is 1 trappable state ($m_F = -1$) for $F = 1$ and 2 for $F = 2$ (that is, $m_F = 1, 2$). How do we control which trappable state the atoms will go to? The order of turning ON/OFF the pump/repump matters when loading the MT. We can selectively load either the state.

- **Repump OFF first** loads to the lower $F = 1$
- **Pump OFF first** loads to the upper $F = 2$

In §1.3, we asked "why choose ^{87}Rb as the trapped species?". Our answer was that for trapping, ^{87}Rb has only **one** trappable state ($m_F = -1$) in its lower hyperfine GS ($F = 1$). Since **trap depth** depends on m_F, having only a **single trappable state** is important.

But what about **rubidium-85**? It's less ideal for trapping, since the $F = 2$ lower level of the GS ($5^2S_{1/2}$) has **two** trappable states. We can remedy this some what, by **gravitational filtering** – used to isolate the $|F = 2, m_F = -2\rangle$ state of ^{85}Rb. How? By lowering the trap depth (by lowering ∇B) so that the $m_F = 1$ state is not supported by gravity, but the $m_F = 2$ state is.

$\mathbf{5^2S_{1/2}}$	$\mathbf{F} = 2$	$\mathbf{g_F} = +\frac{1}{2}$	$\mathbf{m_F} = 1,\ 2$
	$\mathbf{F} = 1$	$\mathbf{g_F} = -\frac{1}{2}$	$\mathbf{m_F} = -1$

Table 3: Allowed states for ^{87}Rb transitions. The Landé factor g_F is also referred to as g_L in previous text.

2.2.3 Trap depth and RF knife

Consider an atom of state m_F in an MT with a **trap depth**, **U**. Along a direction $\hat{n}$, U will be

$$\Delta E = g_F m_F \mu_b (B_{\max} - B_{\min}) \qquad \text{(along a direction } \hat{n}) \tag{24}$$

where $B_{\max}/B_{\min}$ are accessible to the atom, along that direction $\hat{n}$. These values are often constrained by the environment. The limiting factors for a quadrupole field produced by anti-Helmholtz coils are $B_{\min} = 0$ and the size of the vacuum cell, which limits $B_{\max}$ (our case), or the *roll-off*[14] magnetic field. The cell walls are at room temperature and so upon collision, a trapped atom gains K.E. and leaves – note that at the **cell wall**, an atom attains its **maximum energy**.

The magnetic field gradient not isotropic around the field-zero, meaning the trap depth is also **not isotropic** and is direction-dependent. We then conclude that,

> The trap depth U is dependent on the direction $\hat{n}$. Thus, U is defined to be the **average** $\mathbf{E}_{\max}$ of a trapped atom travelling in the downward **axial** $-\hat{\mathbf{z}}$ and **radially** $+\hat{\mathbf{r}}$ outward directions. (Eqn. 25)

Let's formally define some quantities:

- U, the trap depth
- w, the cell wall
- $\hat{z}^{\downarrow}$, the downward axial direction $\hat{z}$ (from field-zero to w) ~ 0.5 cm
- $\hat{r}^{+}$, the radially outward direction (from field-zero to w) ~ 0.5 cm
- $B_w(\hat{n}^j)$, the magnitude of $\vec{B}$ in directions $\hat{n}^j$ at w, where j gives the direction of motion
- $E(B_w(\hat{n}^j))$, the atom energies at w, in directions $\hat{n}^j$

$$k_B U = \frac{\left[E(B_w(z^{\downarrow})) - mgz_w\right] + E(B_w(r^{+}))}{2} \tag{25}$$

If $z^{\downarrow} = 0.5$ cm, then U is $\frac{mgz^{\downarrow}}{k_B} = 0.5$ mK lower for ^{87}Rb. This $mgz^{\downarrow}$ term accounts for the decrease/lowers the trap depth (along $z^{\downarrow}$) by **gravity**. For MTs, trap depths are typically on the order of mK.

In section 1.1.2, we stated the field geometry of a pair of anti-Helmholtz coils. In Appendix C, we gave a more detailed description and used a **multipole expansion**[15]. For simplification, we only kept the terms linear[16] in **r**, which were

$$\frac{\mu_0 I R^2}{2(R^2+a^2)^{3/2}}\hat{z} \qquad \text{and} \qquad \frac{3\mu_0 I a R^2}{2(R^2+a^2)^{5/2}}\left(-\frac{x}{2}, -\frac{y}{2}, z\right) \tag{26}$$

where μ_0 is the permeability of free space and $2a$, the spacing between the coils. Let d be the spacing between the two coils. The coordinates are as in 4b. In §1.1.2, we saw that the maximum field gradient

[14] Here, we take the field roll-off to be a point where the the field drops dramatically, like a ball rolling off a cliff.
[15] VERIFY THIS
[16] A more accurate approach would be to use the magnetic field for a circular loop and keep H.O. terms.

of B_z is given when the coils are placed the coils are placed $d = R$ apart. Consequently,

$$\frac{B(0)}{\partial z} = 2\frac{B(0)}{\partial r} = \frac{48\mu_0 I}{25\sqrt{5}R^2} \tag{27}$$

$$\tag{28}$$

in words,

The predicted gradient along the axial direction is **twice** that in the radial direction.

$\therefore$ The **trap depth** along the axial direction is **twice** that in the radial direction.

RF Knife

In forming the first experimentally observed Bose-Einstein Condensate (BEC), a cloud of rubidium atoms were cooled below the critical temperature using this method [7]. An RF knife is used to control the MT trap depth (while the MT is on). In the figure below, assuming $g_F > 0$, the trappable state is $m_F = 1$ and the untrappable state $m_F = 0$.

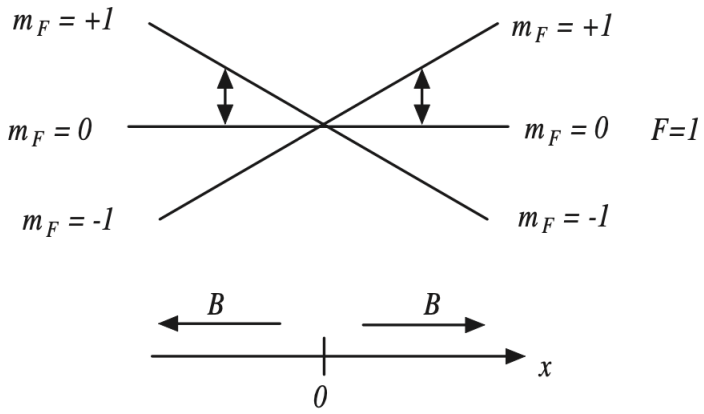

In Figs. 9 and 10, we saw that the transition, in a typical MOT, is on the order of MHz. Why? So that a RF source can be used to drive $m_F = -1 \rightarrow m_F = 1$ transitions. The energies of states $|-1, +1\rangle$ shift in opposite directions, changing the total ΔE between these two states; thus, the $-1 \rightarrow +1$ transition experiences a Zeeman shift.

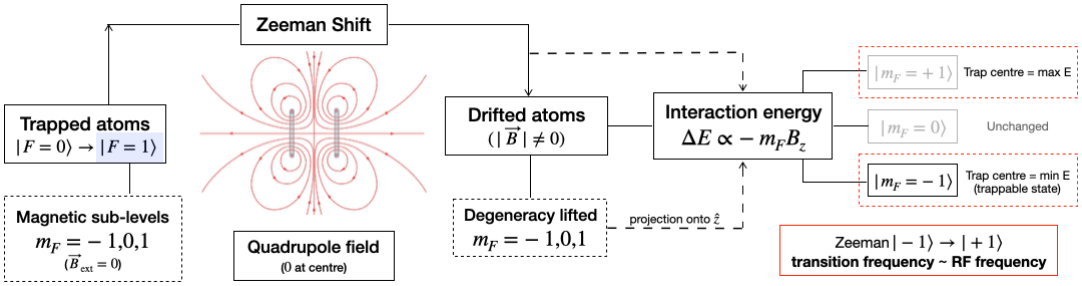

The size of this shift depends on the magnetic field strength, which increases linearly and radially outward from the trap centre. Atoms close to the centre are **cold** and therefore, experience a small Zeeman shift at this transition $\nu\big|_{-1}^{+1}$. Atoms further away are **warm** and in a stronger field and therefore, experience a large Zeeman shift at $\nu\big|_{-1}^{+1}$.

We can tune the $\vec{B}$-field to MHz frequencies to drive the $m_F = -1 \rightarrow m_F = 1$ transition. If atoms experience a Zeeman shift equal to the frequency of the RF source, they are driven to the untrappable state, $|+1\rangle$. This 'cuts out' atoms that experience a larger Zeeman shift, and therefore are warmer and more energetic. The RF knife effectively lowers the walls of the **trapping potential well** and 'trims' the **high-energy tail** of the Maxwell-Boltzmann distribution.

$\Rightarrow$ This limits the $E_{\max}$ an atom can have in the trap and therefore, the trap depth.

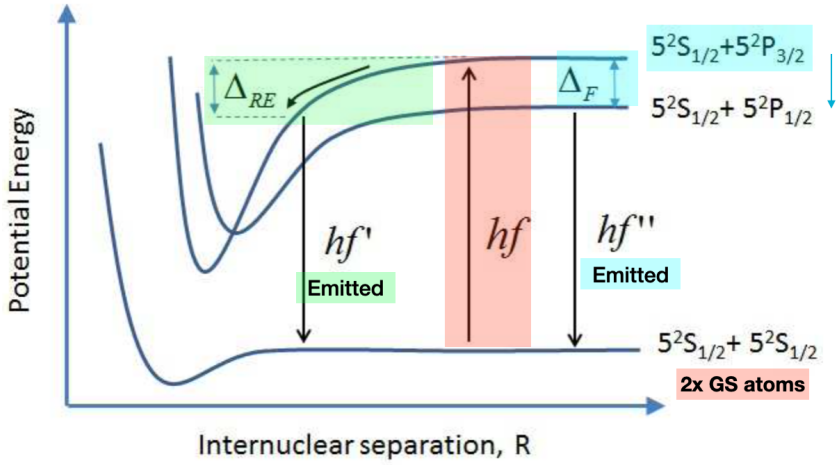

Figure 19: **RE**: 2 (light) GS atoms are excited by a photon of energy hf and gain KE Δ_{RE}, then emit a photon with $hf' < hf$ to return to GS. | **F**: atoms in the $5^2S_{1/2}+5^2P_{3/2}$ ES transfer to the $5^2S_{1/2}+5^2P_{1/2}$ ES and gain KE ΔF, then emit a photon with $hf" < hf$ to return to GS. For homonuclear collisions, each atom gains $\Delta F/2$.

3 Trap Dynamics

3.1 MOT Dynamics

The number of atoms N in a MOT as a function of time t can be given by

$$\frac{dN}{dt} = R - \Gamma N - \beta \int n^2(\vec{r},t) d^3\vec{r} \tag{29}$$

where $N(t=0) = 0$ is when both the $\vec{B}$-field and light have been turned off.

- R, loading rate; the # atoms per second entering the triple beam intersection (rate of capture)
- ΓN, loss due to background collisions
- Γ, loss rate constant (due to background collisions); $[\Gamma] = s^{-1}$ with typical values $\Gamma \sim 0.1 = 2\ \text{s}^{-1}$
- $\tau = 1/\Gamma$, trap lifetime
- $n(\vec{r},t)$ = trapped atom density at position $\vec{r}$ at time t; the origin is the trap centre
- β loss rate constant due to 2-body "intra-trap" collisions; of order $\mathcal{O}(10^{-11} - 10^{-13}\ cm^3 s^{-1}$ Mediated by **radiative escape** ($\Delta\text{RE} = hf' = hf$), and fine ($\Delta F$)/hyperfine changing collisions, where ΔF is the fine structure E split between the $5^2P_{3/2}$ and $5^2P_{1/2}$

Clearly, if the KE $\Delta\text{RE}/F$ gained by an atom is greater than the trap depth, they are lost. For ^{87}Rb , each atom gains $\frac{\Delta F}{2k_B} = 117$ K which is $\gg U_{\text{MOT}} \sim$ several K. Hyperfine changing collisions (i.e. changes in their F level) can also alter their KE – e.g. the ΔE gained by an atom transitioning from $F = 2 \to F = 1$ goes to the KE of the atoms (one or both may change their F level, so as their sum total of m_F remains the same).

For a **low density gas**, $\beta \int n^2(\vec{r},t) d^3\vec{r} \ll \Gamma N$ (i.e. **negligible** compared to the background loss rate term) then the solution (and steady state sol'n) to Eqn. 29 is (as shown in Appendix D)

$$N(t) = \frac{R}{\Gamma}\left(1 - e^{-\Gamma t}\right) \qquad \text{where } N_{\text{SS}}(t=\infty) \to \frac{R}{\Gamma} \sim 10^7 - 10^{10} \text{ atoms} \tag{30}$$

What if we have a **high density gas**, where $\beta \int n^2(\vec{r},t) d^3\vec{r}$ is **non-negligible**, but the atom number

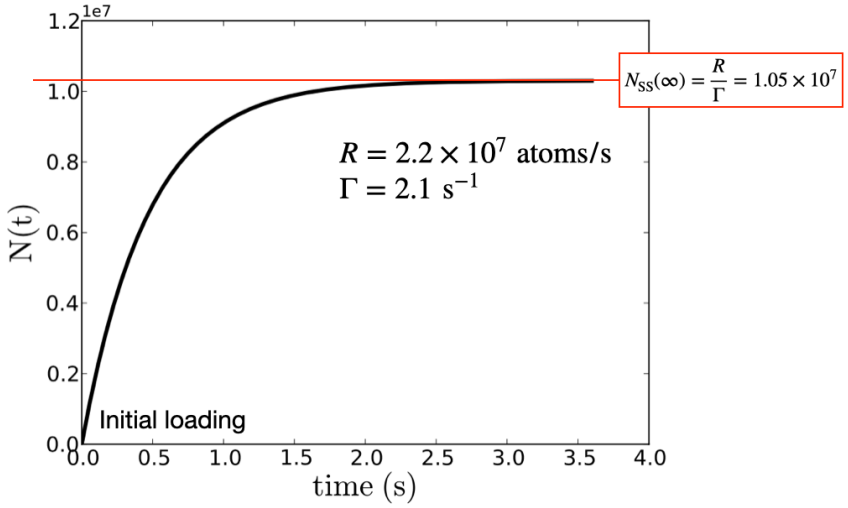

Figure 20: Atom number $N(t)$ vs. time t from initial MOT loading.

density is still $\lesssim 10^{10}$ atoms? Then, the MOT atomic cloud has a **Gaussian density profile**

$$n(\vec{r},t) = n_0(t)e^{-\left(\frac{|\vec{r}|}{w}\right)^2} \tag{31}$$

where $n_0(t)$ is the peak density at $\vec{r}=0$, and w is the (T.I.) width of the distribution. Then,

$$\int n^2(\vec{r},t) = (n_0(t))^2 \left(w\sqrt{\frac{\pi}{2}}\right)^3 \tag{32}$$

and

$$N(t) = \int n(\vec{r},t)dV = n_0(t)\int_V e^{-\left(\frac{|\vec{r}|}{w}\right)^2} r^2 \sin\theta d\theta d\phi dr \tag{33}$$

and $d\theta \in (0,\pi)$ and $d\phi \in (0,2\pi)$ as per usual for polar θ and azimuthal ϕ angles in spherical coordinates. Integrating the density, the total number in the trap is

$$N(t) = n_0(t)\underbrace{\int_0^\infty r^2 e^{-\left(\frac{|\vec{r}|}{w}\right)^2} dr}_{\frac{\sqrt{\pi}}{4}w^2}\underbrace{\int_0^\pi \sin\theta d\theta \int_0^{2\pi} d\phi}_{4\pi} = n_0(t)(w^3\sqrt{\pi}) \tag{34}$$

then Eqn. 29 is now

$$\frac{dN}{dt} = R - \Gamma N - aN^2 \qquad \text{where } a = \frac{\beta}{(w^3\sqrt{\pi})} \tag{35}$$

$$N(t) = N_{SS}\frac{1-e^{-\gamma t}}{1+\zeta e^{-\gamma t}} \qquad \text{where } \gamma = \Gamma + 2\beta n_{SS} \quad \text{and} \quad \zeta = \frac{\beta n_{SS}}{\Gamma + \beta n_{SS}} \tag{36}$$

where the steady state number and average state density are

$$N_{SS} = \frac{R}{\Gamma + \beta n_{SS}} \qquad n_{SS} = \left(\frac{\int n^2 d^3r}{\int n d^3r}\right)_{SS} \tag{37}$$

We'll also include Dr. James booth's derivation below:

$$N(t) = \frac{\gamma - \Gamma}{2a}\frac{1-e^{-\gamma t}}{1-\left(\frac{\Gamma-\gamma}{\Gamma+\gamma}\right)e^{-\gamma t}} \tag{38}$$

What if the density **n is large**? The probability for **multiple scattering**[17] increases. This results in an **outward force** on the trapped atoms – we can think of each atom as having its own '*personal space*' – which sets a limit on the maximum trapped atom density at around $10^{10} - 10^{11}$ cm^{-3} (and the density profile becomes constant[18]). This is not ideal, as this outward force looks like **fluorescence** (as # of γs) decreases due to increased absorption.

Low fluorescence + high background scattered light = bad SNR

Assuming the trapped atom density is a constant n, Eqn. 29 now becomes

$$\frac{dN}{dt} = R - \Gamma N - \beta n N \tag{39}$$

$$N(t) = \frac{R}{\Gamma_{\text{eff}}}\left(1 - e^{-\Gamma_{\text{eff}} t}\right) \qquad \text{where } \Gamma_{\text{SS}} = \Gamma + \beta n \tag{40}$$

3.2 MT Dynamics

MTs are loaded once initially (i.e. for MTs, the loading rate $R = 0$), then decay over time due to background collisional loss. After initial loading, the atom number vs. time is

$$\frac{dN}{dt} = -\Gamma N - \beta \int n^2(\vec{r}, t) d^3\vec{r} - MN \tag{41}$$

where Γ, n, and β are the same as defined above, though the intra-trap term β now includes only hyperfine changing collisions.

> Q: Why doesn't β? ignore fine structure changing collisions in an MT?
> Fine structure changing collisions and radiative escape are not loss mechanisms in MTs, because these processes involve the presence of light.

- M, the loss rate constant due to **Majorana spin flip losses**
  This may occur when a trapped atom passes the $\vec{B} = 0$ point in the quadrupole trap, where $\vec{B}$ changes directions. In this case, the m_F sign can 'flip' and the atom will no longer be trapped.

The decay time due to Majorana spin flips is estimated to be

$$\tau_{\text{decay}} = \frac{ml^2}{3\hbar} \qquad \text{(due to } M\text{)} \tag{42}$$

where m is the trapped atom's mass and l, their radius.

If we assume now that the β (intra-trap) M terms are negligible, then Eqn. 41 has the simple form and solution

$$\frac{dN}{dt} = -\Gamma N \qquad \Rightarrow \qquad N(t) = N(0)e^{-\Gamma t} \tag{43}$$

where $N(0)$ is the initial trapped atom number.

3.3 Background-induced collisional loss

The loss rate constant Γ due to background collisions and its dependence on the trap depth ($\Delta E < U$), background gas density, and collisional loss cross-section, are discussed in terms of their usefulness as a novel **pressure standard**. The elastic collision we're interested in is one between a trapped atom and a background gas atom (from outgassing of vacuum parts, untrapped atoms of the trapped species, or purposefully introduced background gases like Ar, N_2, or He).

We formally define the collisional lost rate constant (Appendix F)

$$\Gamma = \sum_i n_i \langle \sigma_{\text{loss}} v_i \rangle_{X,i} \tag{44}$$

[17] Trapped atoms absorb photons emitted by other trapped atoms.
[18] Here, we're imagining going from a Gaussian distribution to a 'top-hat' distribution.

where the terms are

- i, the background species (e.g. ^{40}Ar)
- X, the trapped species (e.g. ^{87}Rb)
- σ_{loss}, collisional loss cross-section between a trapped atom of type X and a background species of type i
- n_i, density of the background species, i
- v_i, the background gas speed (which really should be v_r, the relative gas speed). $\langle \dots \rangle$ is the Maxwell-Boltzmann average over all speeds ($0 \to \infty$)

As σ_{loss} depends on the depth of the trap, if the trap is anisotropic then the average depth is taken. We say it should be the relative KE, since we're assuming the trapped atoms are in the stationary lab frame w.r.t the background atoms.

3.3.1 Quantum Scattering Theory

The Hamiltonian for 2 interacting particles is

$$H = \frac{|\vec{p}_1|^2}{2m_1} + \frac{|\vec{p}_2|^2}{2m_2} + V\left(|\vec{r}_1 - \vec{r}_2|\right) \tag{45}$$

The centre of mass (COM) coordinate and velocity are

$$\vec{R} = \frac{m_1\vec{r}_1}{M} + \frac{m_2\vec{r}_2}{M} \quad \text{and} \quad \vec{v}_R = \frac{m_1\vec{v}_1}{M} + \frac{m_2\vec{v}_2}{M} \tag{46}$$

where $M = m_1 + m_2$ and $M\vec{v}_R = \vec{p}_1 + \vec{p}_2 = \vec{P}$. Using COM and relative coordinates, we can relate H to the QM operator form

$$H = \underbrace{-\frac{\hbar^2}{2M}\nabla_R^2}_{\text{COM}②} \underbrace{-\frac{\hbar^2}{2\mu}\nabla_r^2}_{\text{REL}①} + V(r) \tag{47}$$

where ∇_R^2 and ∇_r^2 are the laplacian w.r.t COM and relative coordinates, respectively (see Appendix E for the full derivation). We can split the Hamiltonian as $V(r)$ only depends on COM coordinates, $\vec{r}_{1,2}$, and view it as 2 pictures

② 2 particles collide with equal and opposite momentum (free particle term)

① stationary particle (with a spherically symmetric potential) interacts with the reduced mass particle

A solution to the T.I.[19] S.E. $H\psi = E\psi$ with $E = E_r + E_r$ is $\psi = \psi_R\psi_r$, such that the two components of the w.f. satisfy

$$\psi_R: \quad -\frac{\hbar^2}{2M}\nabla_R^2\psi_R = E_R\psi_R \qquad ② \qquad E_R = \frac{P_R^2}{2M} \tag{48}$$

$$\psi_r: \quad \left[-\frac{\hbar^2}{2\mu}\nabla_r^2 + V(r)\right]\psi_r = E_r\psi_r \qquad ① \tag{49}$$

where P_R is the magnitude of the COM momentum. In the COM frame with $P_R = 0$, $E_r = 0$ and $E = E_r$. We now assume that the change in speed (in the lab frame) of the trapped atom due to collision is $\gg$ than the initial speed of the trapped atom before collision. Under this assumption, the KE imparted to the trapped atom with mass m_1 in the lab frame is

$$\Delta E \approx \frac{\mu^2}{m_1}|\vec{v}_r|^2\left(1 - \cos(\theta)\right) \tag{50}$$

(see Fig. 27 in Appendix E). If $\Delta E > U_0$, then the involved atom will be lost. This corresponds to angles of

$$\Delta E > U_0 \qquad \theta_{\min} = \cos^{-1}\left(1 - \frac{U_0 m_1}{\mu_2|\vec{v}_r|^2}\right) \tag{51}$$

Thinking about the COM collision as a single (reduced mass) particle μ approaching a radially symmetric

[19] We use a T.I. treatment here, as a T.D. treatment in [8] gives the same result for the differential cross-section as we'll see later.

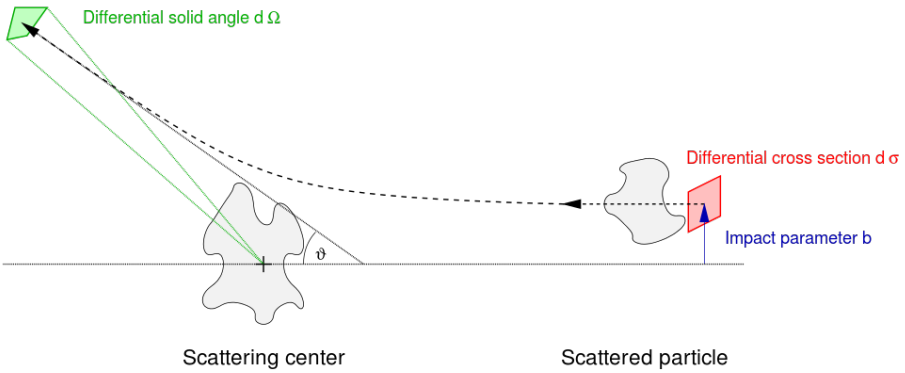

Figure 21: The classical 2-particle scattering process. One particle is scattered on a single scattering centre. The impact parameter b and the differential cross section element $d\sigma$ and the solid angle element $d\Omega$ in the exit direction are as marked. Their quotient is the differential cross section.

potential V that $\to 0$ as $r \to \infty$, then the sol'n ψ_r has the form

$$\psi_r \sim \underbrace{e^{i\vec{k}\cdot\vec{r}}}_{\substack{\text{free particle}\\ \text{plane wave}}} + \underbrace{f(k,\theta,\phi)}_{\substack{\text{scattering}\\ \text{amplitude}}} \underbrace{\frac{e^{ikr}}{r}}_{\substack{\text{spherical}\\ \text{wave}}} \tag{52}$$

to describe the particle far from the potential region post-collision. The probability of scattering into angles θ and ϕ depends on the scattering amplitude, $f(k,\theta,\phi)$ – this indicates that the scattering probability is different between the two directions θ, ϕ. The wavevector $\vec{k}$ is related to the energy of the **relative motion** (i.e. the incident E of the μ-particle, approximated as a free particle far away from the potential region)

$$E_r = \frac{\hbar^2 k^2}{2\mu} \qquad k = \frac{\mu|\vec{v}_r|}{\hbar} \tag{53}$$

We are interested in the case post-collision where the particle is far away from V, s.t. $E_r = E_{\text{incident}}$.

The **classical 2-particle scattering** picture is presented in Fig. 21. A finite width beam of many incoming particles is incident on some target region. A detector collects any scattered particles within a solid angle $d\Omega = \sin\theta d\theta d\phi$, defined the detector area, in a direction (θ, ϕ). The **differential cross-section** is

$$classical: \quad \frac{d\sigma}{d\Omega} = \frac{\Phi \text{ scattered into the direction } \theta,\phi \text{ per unit solid angle}}{\Phi \text{ in the incident beam per unit area}} \tag{54}$$

where Φ is flux with (classical) units $[\Phi] = \#\text{ atoms}/s$. The # of atoms passing through a differential area $d\vec{S}$ is $\vec{J}\cdot d\vec{S}$ where $\vec{J}$ is the **mass current density**, the # of particles passing through dA per dt. With no sources/sinks (particles not created/destroyed), $\vec{J}$ obeys the **continuity equation**

$$\frac{d\rho}{dt} + \vec{\nabla}\cdot\vec{J} = 0 \tag{55}$$

where ρ is the particle density (per dV).

What about the **QM expression** for $\frac{d\sigma}{d\Omega}$? Consider our case of a single particle subject to some localized potential. Then, the probability density[20] $|\psi_r|^2$ can replace the classical density ρ. The units are then $[|\psi_r|^2] = \text{prob./dV}$ and $[\vec{J}] = \text{prob./dAdt}$. Thus, $\vec{J}$ for our μ-particle is

$$\vec{J} = \frac{\hbar}{2\mu i}\left(\psi^*\nabla\psi - \psi\nabla\psi^*\right) = \frac{\hbar}{\mu}\,\text{Im}\left(\psi^*\nabla\psi\right) \tag{56}$$

[20]The probability of finding a particle at a particular place per unit dV, the QM density analogue.

What are the QM versions of the numerator/denominator of Eqn. 54? We can use Eqn. 56 to figure this out

$$\underline{\text{denominator, } d\Omega}: \quad \frac{\vec{J}\cdot d\vec{S}}{dS} = \frac{\hbar k}{\mu} \qquad \begin{cases} \psi_r = e^{ikz} \\ d\vec{S} = dxdy\hat{z} \end{cases}$$

$$\underline{\text{numerator, } d\sigma}: \quad \frac{\vec{J}\cdot d\vec{S}}{d\Omega} = \frac{\hbar k|f(k,\theta,\phi)|^2}{\mu} \qquad \begin{cases} \psi_r = f(k,\theta,\phi)\frac{e^{ikr}}{r} \\ d\vec{S} = r^2\sin\theta d\theta d\phi\hat{r} \end{cases}$$

Taking the ratio gives us the **QM differential cross-section**

$$\frac{d\sigma}{d\Omega} = |f(k,\theta,\phi)|^2 \underbrace{=}_{cyl.sym.} |f(k,\theta)|^2 \tag{57}$$

If we assume **cylindrical symmetry** (which we will from now on), then f isn't a function of ϕ (as shown in the second equality). The **total cross-section** σ is found by integrating over all solid angles $d\Omega$

$$\sigma = \int \frac{d\sigma}{d\Omega}d\Omega = 2\pi\int_0^\pi |f(k,\theta)|^2\sin\theta d\theta \tag{58}$$

Recall Eqn. 44, the definition of Γ, which included the collisional loss cross-section σ_{loss} – but this only includes collisions that induce loss (i.e. $\theta \geq \theta_{\text{min}}$). What's the consequence? It means that instead of starting from $\theta = 0$, we start from $\theta = \theta_{\text{min}}$ (the minimum angle that induces loss). But there are of course heat collisions that don't induce loss, but still have a collisional cross-section. This gives us

$$\sigma_{\text{loss}} = 2\pi\int_{\theta_{\text{min}}}^\pi |f(k,\theta)|^2\sin\theta d\theta \tag{59}$$

$$\sigma_{\text{heat}} = 2\pi\int_0^{\theta_{\text{min}}} |f(k,\theta)|^2\sin\theta d\theta \tag{60}$$

Note that both Eqn. 59 and 60 depend on the relative collision speed through $k = \mu|\vec{v}_r|/\hbar$. For the full derivation of the velocity-averaged collisional loss cross-section $\langle\sigma_{\text{loss}}v_i\rangle_{X,i}$, see Appendix F.

4 Experimental Apparatus and Methods

In [6], ^{87}Rb was used as trapped species X, and ^{40}Ar for background species i. MT depths could be up to 10 mK and measured $\langle\sigma v_{\text{Ar}}\rangle_{^{87}\text{Rb},^{40}\text{Ar}}$ at larger trap depths using a MOT. For a range of trap depths, $\langle\sigma_{\text{loss}}v_i\rangle_{X,i}$was calculated by [9] and [10]. For the optical setup and technical specifications of the **experimental apparatus**, refer to Fig. 22 and Table 4.

4.1 Measurement of $\langle\sigma v_{\text{Ar}}\rangle_{^{87}\text{Rb},^{40}\text{Ar}}$

By measuring Γ at different densities n_{Ar} for a given trap depth, $\langle\sigma v_{\text{Ar}}\rangle_{^{87}\text{Rb},^{40}\text{Ar}}$ can be measured. Different trap depths are achieved by changing the **intensity** and **detuning** of the pump light.

Q: What is the relationship between Γ and n_{Ar}?
As per Eqn. 44, we expect a **linear** relationship between Γ and n_i, with a slope of $\langle\sigma v_{\text{Ar}}\rangle_{^{87}\text{Rb},^{40}\text{Ar}}$.

4.1.1 Γ measurement for a MOT

Fluorescence from trapped atoms in the MOT can be partially captured by a lens and focused onto a photodiode (PD). The **photodiode voltage** $V(t)$ is proportional to the # atoms in the trap $N(t)$ – we assume

$$V(t) = \alpha\gamma_{\text{sc}}N(t) \qquad \alpha \Rightarrow \begin{cases} \text{collecting photons onto PD} \\ \text{conversion of photons to } V \text{ by PD} \end{cases} \tag{61}$$

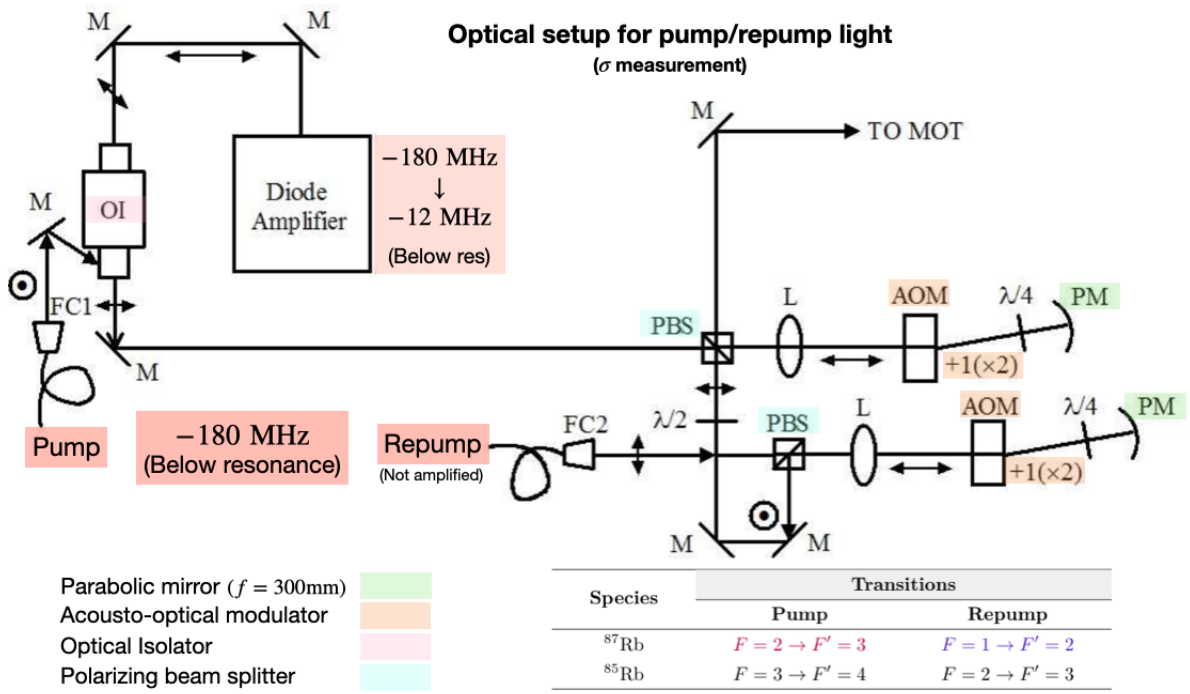

Species	Transitions	
	Pump	Repump
^{87}Rb	$F = 2 \rightarrow F' = 3$	$F = 1 \rightarrow F' = 2$
^{85}Rb	$F = 3 \rightarrow F' = 4$	$F = 2 \rightarrow F' = 3$

Figure 22: Light from the master table was used to inject a diode am- plifier via fiber FC1. An acousto-optical modulator (AOM) in double pass configuraion was used to bring the output of the amplifier from 180 MHz to 12 MHz below the pump resonance. Repump light from fiber FC2 from the master table was also brought up to resonance using an AOM in double pass configuration. The pump and repump beams were combined and sent towards the MOT optics. M: mirror, L: lens (PCX 300 mm). Table 2 included as inset.

Retroflected MOT (6-beam)			
Pump total power	18.3 mW		
Repump total power	0.3 mW		
$1/e^2$ **beam diameter (horizontal/vertical)**	7.0 mm/9.5 mm		
Max. available pump intensity	34.5 mW/cm^2		
B_z **field gradient**	2.79 ± 0.03 T/m		
Glass cell dimensions (under vacuum)	1 cm×1 cm×3.5 cm		
Rb Input		**Ar Bakeout Station**	
Rb dispenser	Alvatec Rb-20	**Turbo, Scroll pump**	TV-70, SH 100 Varian
Ion pump	PS-100 Thermionics	**Residual Gas Analyzer**	RGA200, Stanford Research Systems
Non-evaporable getter	SAES getter	**Ion gauge**	843 Varian
		Leak valve	951-5106 Varian

Table 4: Technical specifications for the setup in [6]. The $1/e^2$ diameter was measured with a Coherent LaserCam-HR beam diagnostic camera. Increases in light intensity would increase MOT atom number until saturation, when light-assisted collisional losses increase and the atom number decreases with increasing intensity. The AOM selects different intensities/detunings to vary trap depth. The RGA was placed about 1 m away from the trapped atoms, taking care to make sure both the RGA and atoms are around 1 m away from the Argon leak valve (to make sure pressure readings between the two correspond). Similarly, the RGA and atoms are also the same distance away from the turbo and scroll pumps. The ion pump is turned off when introducing Argon to minimize pressure differentials between trapped atoms and the RGA.

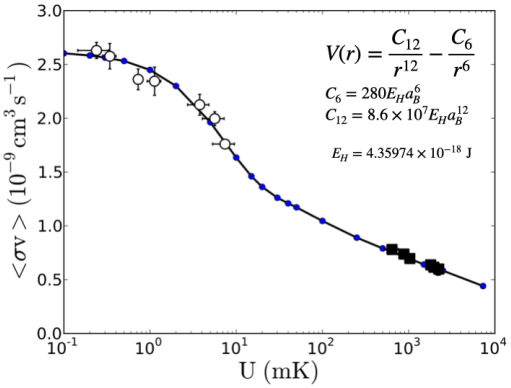

Figure 23: $\langle \sigma v \rangle$ vs. U. As $\uparrow U$, the required KE needed to leave $\uparrow$ and the probability of a collision imparting a sufficient amount of $E \downarrow$. Superimposed points are experimental data and the curve is numerically calculated.

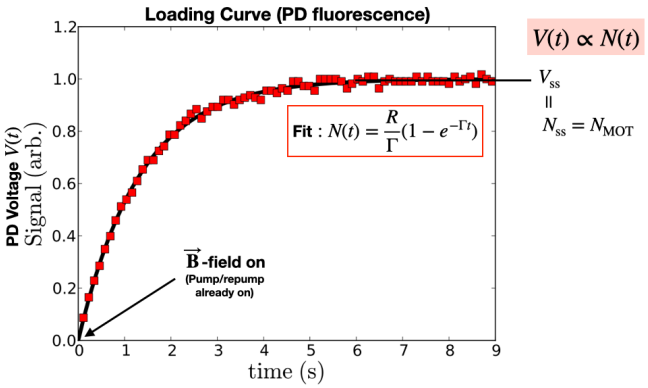

Figure 24: The fluorescence signal of atoms accumulating in a MOT vs. time, from the turn on of $\vec{B}$.

where α is a proportionality constant relating the **collection efficiency** to the **conversion efficiency**. The **scattering rate** γ_{sc} is the rate at which a MOT atom scatters photons (and thus is dependent on light frequency and intensity.) For determining Γ, both α and γ_{sc} are not needed. This is easy to see from the ratio:

$$N_{\text{ss}} = \frac{R}{\Gamma} \qquad V(t) \propto N(t) \qquad \frac{V(t)}{V_{\text{MOT}}}$$

4.1.2 Γ measurement for a MT

An MT is initially loaded by turning OFF the MOT light and $\uparrow \nabla \vec{B}$ (by $\uparrow I$) – the MT starts off with its maximal atom number, which then decays over time as

$$\frac{N(t)}{N(0)} = e^{-\Gamma t} \qquad \frac{V_{\text{MT}}(t)}{V_{\text{MOT}}} \tag{62}$$

where $N(t)$ is the number of atoms after holding for a time t, from an initial loading of $N(0)$ atoms. We can also use the steady state (SS) atom number $N_{\text{MOT}}(t)$ (before loading the MT)

$$\frac{N(t)}{N_{\text{MOT}}} \propto \frac{N(t)}{N(0)} = e^{-\Gamma t} \tag{63}$$

The measurement principle is simple. Recall that for $R = 0$ and $\beta \int n^2(\vec{r}, t) d^3\vec{r}$ negligible, then re-stating from Eqn. 43

$$\frac{dN}{dt} = -\Gamma N \quad \rightarrow \quad N(t) = N(0) e^{-\Gamma t} \qquad \frac{N(t)}{N(0)} = e^{-\Gamma t} \text{ (decay)}$$

Redefining the initial atom #,

$$\frac{N(t)}{N_{\text{MOT}}} \propto \frac{N(t)}{N(0)} = e^{-\Gamma t} \qquad \text{where} \quad \frac{V_{\text{MOT}}^{\text{PD}}(t) = \alpha \gamma_{\text{sc}} N_{\text{MOT}}^{B}}{V_{\text{MOT}}^{\text{PD}}(t) = \alpha \gamma_{\text{sc}} N_{\text{MOT=SS}}} = \frac{N_{\text{MT}}(t)}{N_{\text{MOT}}}$$

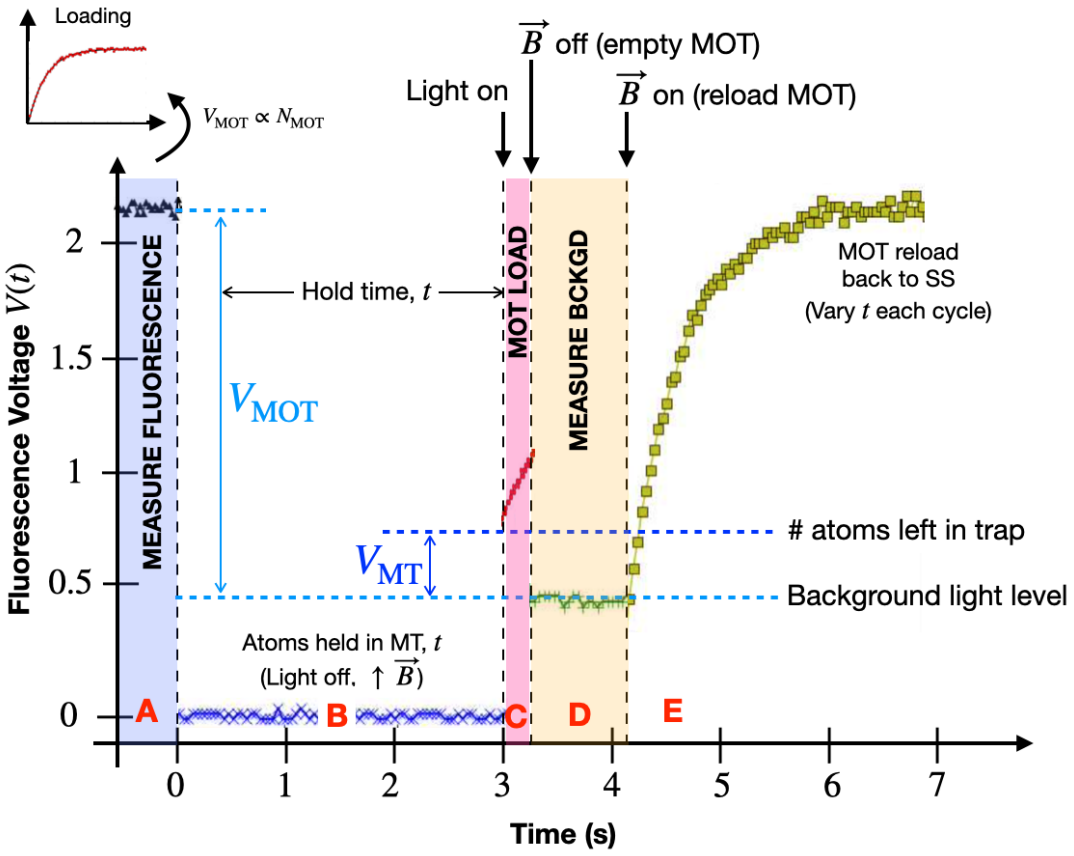

Figure 25: Example data for determining $\frac{N(t)}{N_{\mathrm{MOT}}}$ for a hold time, t. The sequence involves loading the MOT, transferring to the MT, waiting a certain hold time t, and then measuring the fraction $\frac{V_{\mathrm{MT}}(t)}{V_{\mathrm{MOT}}}$.

Experimental Sequence

A Measure fluorescence V from the SS $N(t) \to V_{\text{MOT}} \leftarrow N_{\text{MOT}}$
(Turn ON MOT light and allow it to reach SS fluorescent voltage V_{MOT})

B Turn off light, $\uparrow \vec{B}$ to load trap. Atoms are held from t

C MOT light back ON, $\vec{B} \downarrow$ back to MOT setting
(Turn ON MOT light briefly to check # atoms in trap (by measuring fluorescence. MOT loads briefly during this measurement – this is OK as we can use this line to extrapolate fluorescence – after MOT light is back on. This gives higher voltage than when initially loading the MOT because there are now atoms held in the MOT from the MT, so $\text{MT}_{\text{load}} + \text{MOT}_i > \text{MOT}_i$)

D $\vec{B}$ OFF $\to$ allow trapped atoms to escape. MOT light ON to record background light level
(Empty the MOT by turning OFF the $\vec{B}$-field and measuring background voltage)

E $\vec{B}$ ON to allow MOT to reload completely before returning to step A, varying t with each new cycle
(Reset the MOT – i.e. MOT light still ON, $\vec{B}$ back ON. Repeat, varying the holding time, as we want to characterize Γ)

See Fig. 25.

Q: Why do we need step C?
The MT has no light and atoms don't fluoresce; only background light is detected by the PD. We needed to revert to MOT conditions to detect fluorescence $\to$ # of atoms left. Atoms were held in the MT (from $\uparrow \vec{B}$ to load), so

$$\text{MT}_{\text{load}} + \text{MOT}_i > \text{MOT}_i$$

We only need to do this for a short time (to count MT_{load}), then release trapped atoms ($\vec{B}$) off.

The ratio of interest is

$$\frac{\text{atoms in trap}}{\text{steady state}} = \frac{V_{\text{MT}}(t)}{V_{\text{MOT}}} = \frac{N(t)}{N_{\text{MOT}}} \propto \frac{N(t)}{N(0)} = e^{-\Gamma t} \tag{64}$$

Crucially, this method of trapping assumes that the same fraction of atoms from the MOT are loaded into the MT for each hold-time sequence. This is typically about 50%, and depends on various experimental factors (e.g. trap depth, MOT cloud overlaps with the 0-field point, timing, atom energy states, etc.). By **averaging**, error in Γ and noise can be reduced.

4.1.3 $\langle \sigma v_{\text{Ar}} \rangle_{^{87}\text{Rb},^{40}\text{Ar}}$ Measurement Data

The loss rate constant Γ for the MOT is determined by fitting to a single **loading curve** to a form proportional to $(1 - e^{-\Gamma t})$ as per Eqn. 30. This is seen in Fig. 26 (LHS). Not shown is the error bars for Γ_{MOT} which increase with increasing argon density. This is because the MOT atom # decreases and the loading curve SNR decreases. No error bars were assigned to argon as the calibration error of the residual gas analyzer (RGA) is not known and drifts with time. For the RHS plot of Fig. 26, the MT slope > MOT slope because the MT has a smaller trap depth and thus, the probability of background collisional loss is greater.

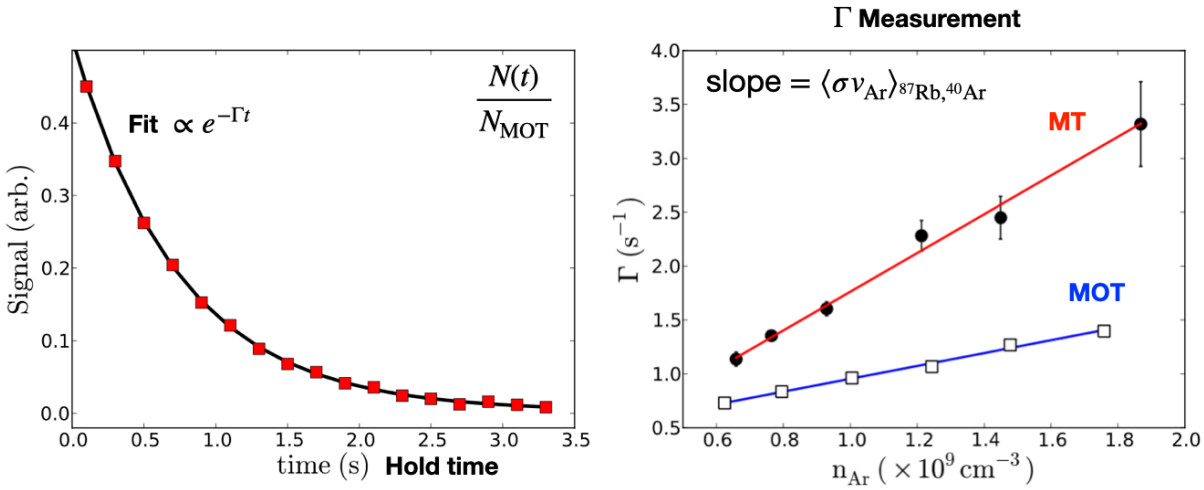

Figure 26: Left: $\frac{N(t)}{N_{\mathrm{MOT}}}$ vs. t fit to $\propto e^{-\Gamma t}$ to extract Γ. | Right: Γ measured for both the MOT and MT as a function of n_{Ar}

References

[1] Min Sung Yoon. *Experiments on magnetic transport, magnetic trapping and Bose-Einstein condensation.* PhD thesis, University of Oxford, 2009.

[2] JGE Harris, RA Michniak, SV Nguyen, WC Campbell, D Egorov, SE Maxwell, LD Van Buuren, and John M Doyle. Deep superconducting magnetic traps for neutral atoms and molecules. *Review of Scientific Instruments*, 75(1):17–23, 2004.

[3] A Corney. Atomic and laser spectroscopy clarendon, 1977.

[4] Daniel A Steck. Rubidium 87 d line data, 2001.

[5] DA Steck. Rubidium 85 d line data, revision 2.1. 6, 20 september, 2013. *URL http://steck. us/alkalidata*, 2013.

[6] Janelle Van Dongen. *Study of background gas collisions in atomic traps.* PhD thesis, University of British Columbia, 2014.

[7] Mike H Anderson, Jason R Ensher, Michael R Matthews, Carl E Wieman, and Eric A Cornell. Observation of bose-einstein condensation in a dilute atomic vapor. *science*, 269(5221):198–201, 1995.

[8] Leonard Sidney Rodberg and Raphael Morton Thaler. Introduction to the quantum theory of scattering. 1967.

[9] David E Fagnan, Jicheng Wang, Chenchong Zhu, Pavle Djuricanin, Bruce G Klappauf, James L Booth, and Kirk W Madison. Observation of quantum diffractive collisions using shallow atomic traps. *Physical Review A*, 80(2):022712, 2009.

[10] David Fagnan. Study of collision cross section of ultra-cold rubidium using a magneto-optic and pure magnetic trap. *Honour Thesis, University of British Columbia*, 2009.

Appendix A Quantum Numbers

Fine Structure ($\vec{L}\cdot\vec{S}$)				**Hyperfine Structure** ($\vec{J}\cdot\vec{I}$)		
$5^2S_{1/2}$	$L=0$	$S=1/2$	$J=1/2$	$J=1/2$	$I=3/2$	$F=\begin{cases}J+I=2\\\lvert J-I\rvert=1\end{cases}$
$5^2P_{3/2}$	$L=1$	$S=1/2$	$J=3/2$	$J=1/2$	$I=3/2$	$F=\begin{cases}J+I=3\\2\\1\\\lvert J-I\rvert=0\end{cases}$

Table 5: Quantum numbers for the energy levels for the D_2 transitions of ^{87}Rb.

Appendix B No local field maximum in MTs

Min/max In univariate calculus, the extremal values of a function can be found by looking at the sign of the second derivative – positive implying concave up, and negative implying concave down. The Hessian matrix contains a matrix of second derivatives.

Eigens Also recall that, when a matrix M acts as a scalar multiplier on a vector X, then that vector is called an eigenvector. The eigenvalue is the factor by which the eigenvector is scaled. In analyzing Hessian matrices, the eigenvalues are important, but the eigenvectors are not. The symmetric property of Hessians have the special property that their eigenvalues will always be real numbers. Thus, we concern ourselves with only the sign $\pm$ of the eigenvalues.

Now, on to magnetic fields/traps. The **Hessian** is a square matrix of second-order partial derivatives of a scalar field. It describes the local curvature of a multivariate function.

$$\mathbf{H}_f = \begin{bmatrix} \frac{\partial^2 f}{\partial x_1^2} & \frac{\partial^2 f}{\partial x_1 \partial x_2} & \cdots & \frac{\partial^2 f}{\partial x_1 \partial x_n} \\ \frac{\partial^2 f}{\partial x_2 \partial x_1} & \frac{\partial^2 f}{\partial x_2^2} & \cdots & \frac{\partial^2 f}{\partial x_2 \partial x_n} \\ \vdots & \vdots & \ddots & \vdots \\ \frac{\partial^2 f}{\partial x_n \partial x_1} & \frac{\partial^2 f}{\partial x_n \partial x_2} & \cdots & \frac{\partial^2 f}{\partial x_n^2} \end{bmatrix}$$

We define a point to be a local extremal point, if one of the following holds:

- **Positive-definite matrix** – a point x is a local **minimum** if the Hessian has all positive eigenvalues at x (concave up).
- **Negative-definite matrix** – x is a local **maximum** if the Hessian has all negative eigenvalues at that point (concave down).
- Saddle point – if the eigenvalues are mixed (i.e. both + and −), it is a saddle point.

A neat property of the Hessian is that the **trace** of the Hessian is equal to the sum of the eigenvalues and is also the **Laplacian** (divergence of a gradient field).

While the second property may be obvious, the first requires a bit more work to prove concretely. Consider a matrix A. We want to find a polynomial whose zeroes are the eigenvalues of A – the characteristic polynomial, $p_A(t)$. For a general matrix A, λ is an eigenvalue of A iff there is a non-zero eigenvector, such that

$$A\mathbf{v} = \lambda\mathbf{v} \quad \text{or} \quad (\lambda I - A)\mathbf{v} = 0$$

The eigenvalues of A are the roots of $\det(\lambda I - A) = 0$ – where $\det(A - \lambda I_n) \neq 0$ is only true iff A is invertible. Let $\mathrm{tr}(A)$ denote the sum of the diagonal elements of A.

$$\text{For a matrix } A = \begin{bmatrix} a & b \\ c & d \end{bmatrix}, \text{ the characteristic polynomial is } p_A(\lambda) = \lambda^2 - \mathrm{tr}(A) + \det(A)$$

More formally, for any $n \times n$ matrix, the characteristic polynomial is given by

$$p_A(\lambda) = (-\lambda)^n + \mathrm{tr}(A)(-\lambda)^{n-1} + \cdots + \det(A)$$

and has exactly n roots and therefore, exactly n eigenvalues when counting multiplicity (and allowing complex eigenvalues).

Proof **Fundamental theory of algebra**
"For a $n \times n$ matrix A, the characteristic polynomial has exactly n roots. There are, therefore, exactly n eigenvalues of A if we count them with multiplicity."

Corollary "Any polynomial P of degree $n \geq 1$

$$P(z) = a_0 + a_1 z + \ldots + a_n z^n, \quad a_n \neq 0 \tag{65}$$

has exactly n roots."

The easiest approach is 'proof by contradiction', together with Liouville's theorem. We would like to show that a polynomial $p(z) = z^n + a_{n-1}z^{n-1} + \ldots + a_1 z + a_0$ always has at least one root z_0. Suppose that $P(z)$ does not have a zero. Then,

1. $f(z) = 1/P(z)$ is entire (obvious from assumption).

   Recall: A complex-valued function f is said to be entire if it is holomorphic on the whole complex plane $\mathbb{C}$. That is, if f is analytic at all finite points on the plane, then it is entire.

2. $f(z)$ is bounded (this follows from $1/P(z) \to 0$ as $|z| \to \infty$. So, $|1/P(z)|$ is bounded by M).

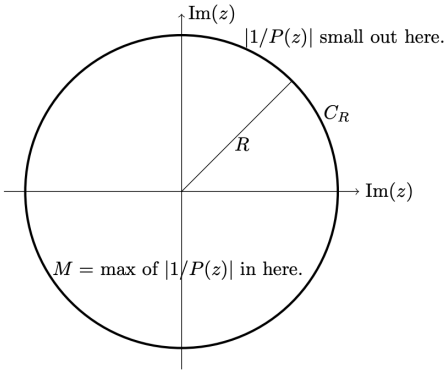

We remind ourselves of a useful theorem in complex analysis, which follows from the fact that holomorphic (differentiable) functions are analytic (power series expansion).

Liouville's theorem "Assume $f(z)$ is entire and bounded in the complex plane, namely $|f(z)| < M \forall\ z \in \mathbb{C}$; then, $f(z)$ is constant." In other words, "If f is entire and bounded, then f is constant."

By Liouville's theorem $f(z)$ is constant and therefore, $P(z)$ must be constant as well. But, this is a contradiction! Our 'no-zeroes' hypothesis must be wrong, and the converse should be true – P must have a zero.

The hard part is over. Now to finish the proof: P has exactly n zeroes.

Let z_0 be one zero. We can factor $P(z) = (z - z_0)g(z)$, where $g(z)$ is a polynomial of degree $(n-1)$. If $(n-1) > 0$, then we can continually apply our above result to $g(z)$ until the degree of g is 0 (induction in n).

Appendix C Deriving the anti-Helmholtz field

We begin with the Biot-Savart law

$$\mathbf{B}(\mathbf{r}) = \frac{\mu_0 I}{4\pi} \int d\mathbf{r}' \times \frac{\mathbf{r} - \mathbf{r}'}{|\mathbf{r} - \mathbf{r}'|^3} \tag{66}$$

where the full displacement vector $\mathbf{r} - \mathbf{r}'$ is measured from the wire element to the point r where we evaluate the field. $d\mathbf{r}'$ is a line integration and I is the current through the wire.

Far from the conductor (i.e. $|\mathbf{r}'| \gg |\mathbf{r}|$), we can perform a **(multipole) series expansion** on the above.

$$\frac{1}{|\mathbf{r} - \mathbf{r}'|^3} = \frac{1}{|\mathbf{r}'|^3} + \frac{3\mathbf{r}\cdot\mathbf{r}'}{|\mathbf{r}'|^5} + \dots$$

$$\mathbf{B}(\mathbf{r}) = \frac{\mu_0 I}{4\pi} \int d\mathbf{r}' \times (\mathbf{r} - \mathbf{r}') \frac{1}{|\mathbf{r}'|^3} + \frac{3\mu_0 I}{4\pi} \int d\mathbf{r}' \times (\mathbf{r} - \mathbf{r}') \frac{\mathbf{r}\cdot\mathbf{r}'}{|\mathbf{r}'|^5} \tag{67}$$

In calculating the field for a anti-Helmholtz (AH) quadrupole trap, we begin with considering a single ring of radius R, shifted vertically as $+a$. The integration coordinate is $\mathbf{r}' = R\cos\theta\hat{x},\ R\sin\theta'\hat{y},\ +a\hat{z}$ with $d\mathbf{r}' = R\hat{\theta}d\theta'$. Consider the following terms needed for computing Eqn. 67

$$\begin{aligned} \hat{\theta} \times (\mathbf{r} - \mathbf{r}') &= (-\sin\theta', \cos\theta', 0) \times (x - R\cos\theta', y - R\sin\theta', -a) \\ &= (-a\cos\theta', -a\sin\theta', R - y\sin\theta' - x\cos\theta') \end{aligned} \tag{68}$$

and

$$\mathbf{r}\cdot\mathbf{r}' = xR\cos\theta' + yR\sin\theta' + za \tag{69}$$

Now, we can use Eqns. 68 and 69 to evaluate the integral in Eqn. 67, keeping only terms the **linear in r**, which are

$$\frac{\mu_0 I R^2}{2(R^2+a^2)^{3/2}}\hat{z} \qquad \text{and} \qquad \frac{3\mu_0 I a R^2}{2(R^2+a^2)^{5/2}}\left(-\frac{x}{2}, -\frac{y}{2}, z\right)$$

Therefore, for the field for this case

$$\mathbf{B}_{+a}(\mathbf{r}) = \frac{\mu_0 I R^2}{2\left(R^2+a^2\right)^{3/2}}\hat{z} + \frac{3\mu_0 I a R^2}{2\left(R^2+a^2\right)^{5/2}}\left(-\frac{x}{2}, -\frac{y}{2}, z\right) \qquad \text{(single ring, shifted by } +a) \tag{70}$$

The field produced by the other ring is then a straightforward mapping of $I \to -I$ and $+a \to -a$,

$$\mathbf{B}_{-a}(\mathbf{r}) = -\frac{\mu_0 I R^2}{2\left(R^2+a^2\right)^{3/2}}\hat{z} + \frac{3\mu_0 I a R^2}{2\left(R^2+a^2\right)^{5/2}}\left(-\frac{x}{2}, -\frac{y}{2}, z\right) \tag{71}$$

and finally, by superposition we arrive at the total field (and potential)

$$\mathbf{B}_{\text{tot}}(\mathbf{r}) \equiv \mathbf{B}_{+a}(\mathbf{r}) + \mathbf{B}_{-a}(\mathbf{r}) = B_0\left(-\frac{x}{2}, -\frac{y}{2}, -z\right) \qquad \text{(total field)} \tag{72}$$

$$B_0 \equiv -\frac{3\mu_0 I a R^2}{2(R^2+a^2)^{5/2}} \qquad \text{and} \qquad U_{\text{mag}}(\mathbf{r}) = g_F m_F \mu_B |\mathbf{B}(\mathbf{r})| \tag{73}$$

Appendix D Solving for $N(t)$

At the beginning of §3.1, we state that the number of atoms $N(t)$ in the trap as a function of time t can be described by

$$\frac{dN}{dt} = R - \Gamma N - \beta \int n^2(\vec{r}, t) d^3\vec{r} \tag{74}$$

and, under the assumption of a low density gas (i.e. $\int n^2(\vec{r}, t) d^3\vec{r}$ is negligible), the corresponding solution

$$N(t) = \frac{R}{\Gamma}\left(1 - e^{-\Gamma t}\right) \tag{75}$$

Let's pause briefly and prove this to ourselves:

$$y' = \frac{dN}{dt} = R - \Gamma N - \beta \cancel{\int n^2(\vec{r}, t) d^3\vec{r}} \qquad \text{Form: } \; y' + q(t)y = C$$

Integrating Factor

Recall that an integrating factor is a function $\mu(t)$ that, when an ordinary differential equation (ODE) is multiplied by, makes it integrable. Here's an example of solving a simple first-order ODE:

$$\frac{dy}{dt} + q(t)y(t) = p(t)$$

where $q(t)$ and $p(t)$ are continuous functions. This can be made integrable by defining a function

$$\mu(t) = \int q(t)dt \quad \text{and} \quad \frac{d\mu}{dt} = q(t)$$

Let $e^{\mu(t)}$ be the integrating factor s.t. multiplying $y(t)$ gives

$$\begin{aligned} \frac{d}{dt}\left[e^{\mu(t)}y(t)\right] &= e^{\mu(t)}\left[\frac{dy}{dt} + q(t)y(t)\right] \\ &= e^{\mu(t)}p(t) \end{aligned}$$

Finally, the solution takes the form

$$y(t) = e^{-\mu(t)} \int e^{\mu(t)}p(t)dt$$

Continuing,

$$\begin{aligned} N' + \Gamma N &= R \\ N'e^{\Gamma t} + \Gamma N e^{\Gamma t} &= Re^{\Gamma t} \end{aligned} \qquad \big) \times \mu(t) = e^{\int q(t)dt} = e^{\Gamma t}$$

Chain rule,

$$\begin{aligned} \left(Ne^{\Gamma t}\right)' = N'e^{\Gamma t} + \Gamma N e^{\Gamma t} &= Re^{\Gamma t} \\ Ne^{\Gamma t} + C_1 &= \tfrac{R}{\Gamma}e^{\Gamma t} + C_2 \end{aligned} \qquad \big) \int$$

$$\begin{aligned} Ne^{\Gamma t} &= \tfrac{R}{\Gamma}e^{\Gamma t} + C_3 \\ N = \tfrac{R}{\Gamma} + \tfrac{C_3}{e^{\Gamma t}} \qquad C_3 &= C_2 - C_1 \end{aligned} \qquad \big) \div e^{\Gamma t}$$

Initial conditions $N(t = 0) = 0$ gives $C_3 = -\frac{R}{\Gamma}$, and finally

$$N(t) = \frac{R}{\Gamma}\left(1 - e^{-\Gamma t}\right) \; \ldots \text{done!}$$

Appendix E 2-particle scattering

The 2-particle interacting Hamiltonian is given by

$$H = \frac{|\vec{p}_1|^2}{2m_1} + \frac{|\vec{p}_2|^2}{2m_2} + V\left(|\vec{r}_1 - \vec{r}_2|\right) \tag{76}$$

and it is useful to define the relative coordinates

$$\vec{r} = \vec{r}_1 - \vec{r}_2 \qquad \text{and} \qquad \vec{v}_r = \vec{v}_1 - \vec{v}_2$$

Under conservation of momentum, $|\vec{v}_r| = |\vec{v}_1\vec{v}_2| = \text{const}$ before and after collision (though its direction does change). If we view the collision in the COM frame, this is evident as the speeds of the particles is unchanged in an **elastic** collision. In the COM frame, $\vec{v}_R = 0$ and the $\vec{P} = 0$ as the particles have equal and opposite momenta. Recalling the momentum operator (in 3D), $\hat{p} = -i\hbar\nabla$, we write (while

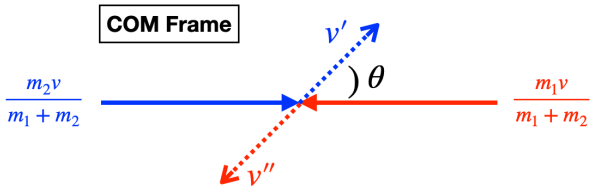

dropping vector notation out of ~~laziness~~ efficiency)

$$\begin{aligned}
\frac{|\vec{p_1}|^2}{2m_1} + \frac{|\vec{p_2}|^2}{2m_2} &= \frac{p_1^2 m_2 + p_2^2 m_1}{2m_1 m_2} = \frac{(p^2 - 2p_1p_2 - p_2^2)m_2 + p_2^2 m_1}{2m_1 m_2} \qquad p^2 = p_1^2 + 2p_1p_2 + p_2^2 = p_R^2 \\
&= \frac{p^2}{2m_1}\frac{(m_1+m_2)m_1}{(m_1+m_2)m_1} - \frac{p_1p_2}{m_1} + \frac{p_2^2(m_1-m_2)}{2m_1m_2} \\
&= \underbrace{\frac{p^2}{2M}}_{\text{COM}} + \underbrace{\frac{(p_1^2 + 2p_1p_2 + p_2^2)(m_1m_2)}{2Mm_1^2} - \frac{p_1p_2}{m_1} + \frac{p_2^2(m_1-m_2)}{2m_1m_2}}_{\text{REL}(*)}
\end{aligned}$$

$$\begin{aligned}
(*) \rightarrow \quad & \frac{p_1^2 m_2}{2Mm_1} + \frac{p_1p_2m_2}{2Mm_1} - \frac{p_1p_2}{m_1} + \frac{p_2^2m_2}{2Mm_1} + \frac{p_2^2(m_1-m_2)}{2m_1m_2} \\
&= \frac{p_1^2m_2^2 + \cancel{p_1p_2m_2^2} - p_1p_2 2(m_1 + \cancel{m_2})m_2 + p_2^2m_2^2 + p_2^2(m_1-m_2)(m_1+m_2)}{2Mm_1m_2} \\
&= \frac{(m_1m_2)^{\cancel{2}}\left[v_1^2 - 2v_1v_2 + v_2^2\right]}{2M\cancel{m_1m_2}} \cdot \frac{\mu}{\mu} \qquad p_r^2 = \mu^2(v_1 - v_2)^2 \\
&= \frac{p_r^2}{2\mu} \qquad \mu = \frac{m_1m_2}{m_1+m_2} = \frac{m_1m_2}{M}
\end{aligned}$$

Putting it all together (and substituting for the momentum operator $p \rightarrow \hat{p} = -i\hbar\nabla$),

$$\frac{|\vec{p_1}|^2}{2m_1} + \frac{|\vec{p_2}|^2}{2m_2} \quad \longrightarrow \quad \frac{p^2}{2M} + \frac{p_r^2}{2\mu}$$

$$= \boxed{-\tfrac{\hbar^2}{2M}\nabla_R^2 - \tfrac{\hbar^2}{2\mu}\nabla_r^2}$$

where ∇_R^2 and ∇_r^2 are the laplacian w.r.t COM and relative coordinates, respectively.

Now, we ask the question:

"What is the KE imparted onto the trapped atom (in the lab frame)?"

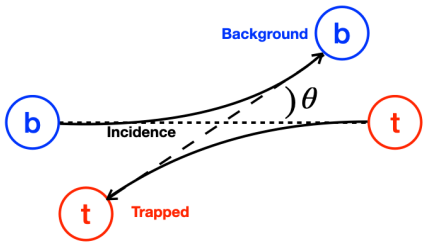

Figure 27: 2 particles in the COM frame travel with equal and opposite momenta. Post-collision, they travel along a line of angle θ w.r.t the original line of incidence.

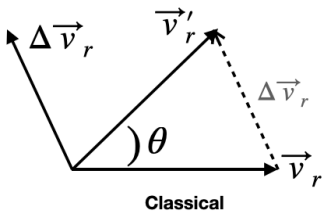

Figure 28: Classical picture.

Start by assuming that $\Delta v_t' \gg v_t$ (in the lab FoR). We need the quantity $|\Delta\vec{v}_r|^2$ for $\Delta E_t \ldots$

$$\begin{aligned}\text{(E. consv)} \qquad & m_t|v_r|^2 + m_b|v_r|^2 = m_t|v_r{}'|^2 + m_b|v_r{}'|^2 \\ & |v_r|^2(m_t + m_b) = |v_r{}'|^2 v(m_t + m_b)\end{aligned}$$

$$\Rightarrow |\vec{v}_r'| = |\vec{v}_r'|$$

The change in the relative velocity

$$\begin{aligned}|\Delta\vec{v}_r|^2 &= |\vec{v}_r - \vec{v}_r{}'|^2 = |\vec{v}_r|^2 + |\vec{v}_r{}'|^2 - 2|\vec{v}_r \cdot \vec{v}_r{}'| \\ &= 2|\vec{v}_r|^2 - 2|\vec{v}_r|^2\cos\theta \\ &= 2|\vec{v}_r|^2(1 - \cos\theta)\end{aligned}$$

We also need $|\Delta\vec{v}_t|$ for $\Delta E_t \ldots$

$$\text{① } \Delta v_t = \Delta v_b - \Delta v_r \qquad \text{② } m_b\Delta v_b = -m_t\Delta v_t \quad \text{(consv. P)}$$

$$\Delta v_b = -\frac{m_t}{m_b}\Delta v_t$$

$$\Delta v_t = -\frac{1}{1 + \frac{m_t}{m_b}}\Delta v_r = -\frac{\mu}{m_t}\Delta v_r$$

where

$$\mu = \frac{m_t m_b}{m_t + m_b} \qquad \frac{1}{1 + \frac{m_b}{m_t}}\frac{m_b}{m_b} = \frac{m_b}{m_t + m_b} = \frac{\mu}{m_t}$$

Therefore, the **change in a trapped atom's E for a given θ** is

$$\Delta E_t(\theta) = \frac{1}{2}m_t\left[\underbrace{|v_t + \Delta v_t|^2}_{\text{Final}} - \underbrace{|v_t|^2}_{\text{Initial}}\right] \tag{77}$$

which after applying our initial assumption of $|\Delta v_t| \gg |v_t|$, simplifies to

$$\therefore \boxed{\Delta E_t(\theta) \approx \tfrac{\mu^2}{m_t}|v_r|^2\,(1 - \cos\theta)} \tag{78}$$

Appendix F Deriving $\langle\sigma_{\text{loss}}v_i\rangle_{X,i}$

We would like to obtain the expression for the *velocity averaged collisional cross-section*,

$$\langle\sigma_{\text{loss}}v_i\rangle_{X,i} = 4\pi\left(\frac{m_i}{2\pi k_B T}\right)^{3/2}\int_0^\infty v_i^3 e^{-\frac{m_i v_i^2}{2k_B^T}}\sigma_{\text{loss}}\left(\frac{\mu\,|v_i|}{\hbar}\right)dv_i \tag{79}$$

which we note is the loss cross-section for collisions that do not involve heat (σ_{heat}). From Eqn. 59, the calculation involves the **scattering amplitude** $f(k,\theta)$, but what is its value?

We begin by writing the sol'n Eqn. 52 in terms of **spherical coordinates** and $\hat{\mathbf{L}}^2$ (angular momentum operator), which satisfies

$$\frac{\hbar}{2\mu}\left[-\frac{1}{r^2}\frac{\partial}{\partial r}\left(r^2\frac{\partial\psi_r}{\partial r}\right)+\frac{\hat{\mathbf{L}}^2}{r^2}\psi_r\right]+V(r)\psi_r=E\psi_r \tag{80}$$

Recall that the separated sol'n is comprised of both radial and angular parts, as

$$\psi_r(r,\theta,\phi)=R_l(r)\underbrace{Y_{l,m}(\theta,\phi)}_{\substack{\text{spherical}\\ \text{harmonic}}} \tag{81}$$

The spherical harmonic $Y_{l,m}(\theta,\phi)$ is an **eigenfunction of $\hat{\mathbf{L}}^2$** with **eigenvalues**

$$\hat{\mathbf{L}}^2 \quad\longrightarrow\quad \hbar^2\ell(\ell+1) \tag{82}$$

(see Appendix G). Substituting in the sol'n $\hat{L}Y_{l,m}=l(l+1)Y_{l,m}$ to ψ_r gives

$$\frac{1}{r^2}\frac{d}{dr}\left(r^2\frac{dR_l}{dr}\right)-\frac{l(l+1)}{r^2}R_l+\frac{2\mu}{\hbar^2}[E-V(r)]R_l=0 \tag{83}$$

The spherical harmonics are proportional to the **Legendre polynomials** $Y_{l,0}(r,\theta)\propto P_l(\cos\theta)$, so we take linear combinations (LCs) for the most general sol'n

$$\psi_r(r,\theta)=\sum_{l=0}^{\infty}(2l+1)i^lA_lR_l(r)P_l(\cos\theta) \tag{84}$$

where for a free particle, we can immediately say $A_l=1$; else, it must be determined.

Appendix G *Review:* Spherical Harmonics

Let's begin with Laplace's equation in spherical coordinates

$$\begin{aligned}\nabla^2V&=0\\ \nabla^2V&=\frac{1}{r^2}\frac{\partial}{\partial r}\left(r^2\frac{\partial V}{\partial r}\right)+\frac{1}{r^2\sin\theta}\frac{\partial}{\partial\theta}\left(\sin\theta\frac{\partial V}{\partial\theta}\right)+\frac{1}{r^2\sin^2\theta}\left(\frac{\partial^2V}{\partial\phi^2}\right)\end{aligned} \tag{85}$$

where θ and ϕ are the usual polar and azimuthal angles. In our atomic cloud, we can assume azimuthal symmetry s.t. $\frac{\partial V}{\partial\phi}=0$ or equivalently, that parameter V does not vary in the ϕ direction. Under this assumption, the above becomes

$$\nabla^2V=\frac{1}{r^2}\frac{\partial}{\partial r}\left(r^2\frac{\partial V}{\partial r}\right)+\frac{1}{r^2\sin\theta}\frac{\partial}{\partial\theta}\left(\sin\theta\frac{\partial V}{\partial\theta}\right)=0 \tag{86}$$

This is the form of Laplace's equation that we would have to solve to find the electric potential in spherical coordinates. *Separation of variables* gives our split solution

$$V = R(r)\Theta(\theta) \qquad \begin{cases} \frac{\partial V}{\partial r} = R'(r)\Theta(\theta) \\ \frac{\partial V}{\partial \theta} = R(r)\Theta'(\theta) \end{cases}$$

Substituting into 86, multiplying by r^2, and dividing by $V = R(r)\Theta(\theta)$ yields

$$\nabla^2 V = \frac{1}{R(r)}\frac{d}{dr}\left(r^2 R'(r)\right) + \frac{1}{\Theta(\theta)\sin\theta}\frac{d}{d\theta}\left(\sin\theta\Theta'(\theta)\right) = 0 \tag{87}$$

The two terms above are ODEs, one a function of r and the other θ, and are both equal to a constant. Separating...

$$\frac{1}{R(r)}\frac{d}{dr}\left(r^2 R'(r)\right) = \ell(\ell+1)$$
$$\frac{1}{\Theta(\theta)\sin\theta}\frac{d}{d\theta}\left(\sin\theta\Theta'(\theta)\right) = -\ell(\ell+1)$$

Two natural questions arise:

1. Why did we choose the separation constant to be $\ell(\ell+1)$?
   Since we know with forethought that this form will produce a well-known diff. eq. whose sol'n we already know.
2. Why do the radial and angular constants differ by a sign?
   This is necessary so that $\sum(\text{equations}) = 0$, as required by Laplace's equation.

The Radial Equation

Solve using Euler's method to get

$$r^2\frac{d^2R}{dr^2} + 2r\frac{dR}{dr} - R\ell(\ell+1) = 0 \qquad \Rightarrow \qquad \therefore\ R(r) = Ar^{\ell} + Br^{-\ell(\ell+1)}$$

where the inset below gives the explicit calculation (should I hit my head on something and forget).

Euler's (Cauchy) Equations
The second order diff. eq. is

$$x^2y'' + 2xy' - \ell(\ell+1)R = 0$$

Assume $y = x^{\ell}$, where ℓ is some constant, the derivatives of which are

$$y' = \ell x^{\ell-1} \qquad y'' = \ell(\ell-1)x^{\ell-2}$$

Thus,

$$\ell(\ell-1)x^{\ell-2} + \frac{2}{x}x^{\ell-1} - \frac{\ell(\ell+1)}{x}x^{\ell}$$
$$x^{-(\ell+1)}\left[\ell(\ell-1) + 2\ell\right] - \ell(\ell+1)x^{\ell} = 0$$

which generalizes to

$$\therefore \quad y(x) = Ax^{\ell} + Bx^{-(\ell+1)}$$

where A and B are constants determined by the boundary conditions (B.C.).

The Angular Equation

Similarly,

$$\frac{d^2\Theta}{d\theta^2} + \frac{\cos\theta}{\sin\theta}\frac{d\Theta}{d\theta} + \ell(\ell+1)\Theta = 0$$

where we've eliminated the term associated with $\frac{\partial^2 V}{\partial \phi^2}$ due to symmetry. Had we not made this assumption, the angular sol'n (called Φ here to differentiate between θ and ϕ coordinates[21]) would be of the form

$$\frac{1}{\Theta}\left[\sin\theta\frac{d}{d\theta}\left(\sin\theta\frac{d\Theta}{d\theta}\right)\right] + \ell(\ell+1)\sin^2\theta = m^2$$

$$\frac{1}{\Phi}\frac{d^2\Phi}{d\phi^2} = -m^2$$

where $\ell(\ell+1)$ and m^2 separation constants. The sol'ns to the angular equations with *spherically symmetric* B.C. are (remembering that $e^{ix} = \cos x + 2\sin x = 1$ and $x = 2\pi m$)

$$\frac{d^2\Phi}{d\phi^2} = -m^2\Phi \quad \Rightarrow \quad \Phi(\phi + 2\pi) = \Phi(\phi) \quad *$$

$$e^{im(\phi+2\pi)} = e^{im\phi}$$

$$e^{im2\pi} = 1 \quad \text{(only true when } m = 0, \pm1, \pm2, \dots\text{)}$$

* i.e. the w.f. must be single-valued (unique) everywhere in space.

The angular equation is known as the **Legendre equation** and has the sol'n

$$\Theta(\theta) = AP_\ell{}^m(\cos\theta) \tag{88}$$

where $P_\ell{}^m$ are the associated **Legendre functions** and $P_\ell(x)$ is the ℓ^{th} **Legendre polynomial**

$$P_\ell{}^m = (1-x^2)^{|m|/2}\left(\frac{d}{dx}\right)^{|m|} P_\ell(x) \qquad \begin{cases} P_0(x) = 1 \\ P_1(x) = \frac{1}{2}\frac{d}{dx}(x^2-1) = x \\ P_2(x) = \frac{1}{2}(3x^2-1) \\ \quad\vdots \end{cases}$$

which is defined by **Rodrigues' formula**:

$$P_\ell(x) = \frac{1}{2^\ell \ell!}\left(\frac{d}{dx}\right)^{|m|}\left(x^2-1\right)^\ell \tag{89}$$

The product of Θ and Φ occurs so frequently in QM that it is known as a **spherical harmonic**

$$Y_\ell{}^m(\theta,\phi) = \epsilon\sqrt{\frac{2\ell+1}{4\pi}\frac{(\ell-|m|)!}{(\ell+|m|)!}}e^{im\phi}P_\ell{}^m(\cos\theta) \qquad \epsilon = \begin{cases}(-1)^m & m \geq 0 \\ 1 & m \leq 0\end{cases} \tag{90}$$

otherwise called *normalized angular functions*, which obey **orthonormality**

$$\int_{\theta=0}^{\pi}\int_{\varphi=0}^{2\pi} Y_\ell^m Y_{\ell'}^{m'*} d\Omega = \delta_{\ell\ell'}\delta_{mm'}$$

We can now write the complete (general) solution of Laplace's equation in spherical coordinates as

$$V(r,\theta) = \sum_{\ell=0}^{\infty}\left(A_\ell r^\ell + B_\ell r^{-(\ell+1)}\right)P_\ell(\cos\theta) \tag{91}$$

[21] We note that in changing the symbol for the θ and ϕ components, the partial derivatives become full derivatives. Written in the natural form $\Theta(\theta,\phi)$, these terms would remain partial derivatives.